

N71-34117  
NASA CR-121856

PROGRESS REPORT (B)  
Grant NGL 34-002-047  
April 2, 1971

"STUDY OF  
RECTANGULAR-GUIDE-LIKE STRUCTURES FOR  
MILLIMETER WAVE TRANSMISSION"

to  
The National Aeronautics and Space  
Administration, Washington, D. C.



CASE FILE  
COPY

DEPARTMENT OF ELECTRICAL ENGINEERING  
NORTH CAROLINA STATE UNIVERSITY  
RALEIGH, NORTH CAROLINA

PROGRESS REPORT (B)  
Grant NGL 34-002-047  
April 2, 1971

"STUDY OF  
RECTANGULAR-GUIDE-LIKE STRUCTURES FOR  
MILLIMETER WAVE TRANSMISSION"

to  
The National Aeronautics and Space  
Administration, Washington, D. C.

North Carolina State University  
Raleigh, North Carolina

Submitted: \_\_\_\_\_

*FJ Tischer*

Dr. Frederick J. Tischer, Professor  
Principal Investigator



## SUMMARY

This report represents the final report on work carried out under Grant NGL 34-002-047 during the period ending June 30, 1971. The report deals with the electromagnetic field structure of the fence guide for frequencies between 12 and 18 GHz. The study was carried out by Robert A. Kraft under the direction of Dr. Frederick J. Tischer as dissertation research for the degree of Master of Science at the North Carolina State University, Raleigh, North Carolina.

#### ABSTRACT

KRAFT, ROBERT ALLEN. Electromagnetic Field Structure of the Fence Guide. (Under the direction of FREDERICK JOSEPH TISCHER).

An evaluation of the propagation characteristics of the fence guide is made using data obtained from field measurements. Changes of these propagation characteristics caused by dielectric loading are investigated. Two prototype guides with several loading configurations were studied. A new technique in automated field-probe measurements is used to obtain very accurate field-distribution plots.

## TABLE OF CONTENTS

	Page
LIST OF TABLES . . . . .	v
LIST OF FIGURES . . . . .	vi
1. INTRODUCTION . . . . .	1
2. LITERATURE SURVEY . . . . .	2
2.1 Introduction . . . . .	2
2.2 H-Guide . . . . .	2
2.3 Wire Grids . . . . .	3
2.4 Fence Guide . . . . .	4
3. EXPERIMENTAL MEASUREMENT TECHNIQUES . . . . .	6
3.1 Introduction . . . . .	6
3.2 Waveguide . . . . .	7
3.2.1 Fence Guide . . . . .	7
3.2.2 Actual Prototype . . . . .	8
3.3 Description of Equipment . . . . .	15
3.3.1 General Test Equipment . . . . .	15
3.3.2 Special Equipment . . . . .	15
3.3.2.1 The Probe . . . . .	15
3.3.2.2 Graphing Equipment and Techniques . . . . .	22
3.4 Q-Value Measurement Techniques . . . . .	22
3.5 Mode Distribution Measurements . . . . .	24
3.6 Field Measurements . . . . .	26
4. MEASUREMENTS . . . . .	27
4.1 Introduction . . . . .	27
4.2 Longitudinal Characteristics . . . . .	28
4.2.1 Introduction . . . . .	28
4.2.2 Determination of $\lambda_g$ . . . . .	28
4.2.3 Relationship of Q- Value and $\alpha_z$ . . . . .	30
4.2.4 Evaluation of $\alpha_z$ . . . . .	31



## TABLE OF CONTENTS (continued)

	Page
4.3 Evaluation of $\alpha_x$ . . . . .	37
4.4 Measurement of lateral leakage . . . . .	71
5. CONCLUSION . . . . .	
5.1 Summary . . . . .	
5.2 Findings . . . . .	
6. LIST OF REFERENCES . . . . .	

## LIST OF TABLES

	Page
4.1 Values of $d$ for insert configurations . .	32
4.2 Mode numbers and their frequencies for the configurations . . . . .	33
4.3 Q-Values . . . . .	34
4.4 Computed values of $\alpha_z$ in dB/cm . . . . .	36
4.5 $\alpha_x$ for various insert configurations . .	40
4.6 Energy leakage . . . . .	72

## LIST OF FIGURES

	Page
3.1 Basic fence guide and coordinate system . .	9
3.2 Field distribution . . . . .	10
3.3 Dimensions of prototype guide . . . . .	11
3.4 General purpose measurement setup . . . . .	13
3.5 Prototype guide, narrow spacing . . . . .	14
3.6 Prototype guide, wide spacing with probe .	14
3.7 Compensated-dipole probe . . . . .	14
3.8 Prototype guides with dielectric inserts .	14
3.9 Probe dimensions . . . . .	16
3.10 Probe with compensation cavity in front of open guide at 13.4 GHz. . . . .	18
3.11 Probe without compensation cavity in front of open guide at 13.4 GHz. . . . .	19
3.12 Probe with compensation cavity in front of open guide at 17 GHz. . . . .	20
3.13 Probe without compensation cavity in front of open guide at 17 GHz. . . . .	21
3.14 Test-bench setup for Q-value and mode- distribution measurements . . . . .	23
3.15 Test-bench setup for field measurements with probe . . . . .	25
4.1 Guide wavelength vs. frequency for the various configurations in the wide guide .	29
4.2 Guide wavelength vs. frequency for the various configurations in the narrow guide . . . . .	29
4.3 Correction factor C vs. $d/\lambda_0$ with $\epsilon_r$ as parameter . . . . .	35
4.4 Vertical field decrease $\alpha_x$ . . . . .	38



## LIST OF FIGURES (continued)

	Page
4.5 Vertical field decrease $\alpha_x$ . . . . .	39
4.6 Longitudinal distribution, wide spacing, empty guide, $f=17.47$ GHz (probe centered)	41
4.7 Longitudinal distribution, wide spacing, empty guide, $f=17.47$ GHz (probe next to fence) . . . . .	42
4.8 Longitudinal distribution, wide spacing, 2xl/16 inserts, $f=17.36$ GHz (probe centered) . . . . .	43
4.9 Longitudinal distribution, wide spacing, 2xl/16 inserts, $f=17.36$ GHz (probe next to fence) . . . . .	44
4.10 Longitudinal distribution, wide spacing, round inserts, $f=17.29$ GHz (probe centered).	45
4.11 Longitudinal distribution, wide spacing, round inserts, $f=17.29$ GHz (probe next to fence). . . . .	46
4.12 Longitudinal distribution, wide spacing, laminated guide, $f=17.41$ GHz (probe centered) . . . . .	47
4.13 Longitudinal distribution, wide spacing, laminated guide, $f=17.41$ GHz (probe next to fence) . . . . .	48
4.14 Longitudinal distribution, narrow spacing, empty guide, $f=17.47$ GHz (probe centered) .	49
4.15 Longitudinal distribution, narrow spacing, 2xl/16 inserts, $f=17.39$ GHz (probe centered) . . . . .	50
4.16 Longitudinal distribution, narrow spacing, 2xl/16 inserts, $f=17.39$ GHz (probe next to fence) . . . . .	51
4.17 Longitudinal distribution, narrow spacing, round inserts, $f=17.1$ GHz (probe centered).	52

## LIST OF FIGURES (continued)

	page
4.18 Longitudinal distribution, narrow spacing, round inserts, $f=17.1$ GHz (probe next to fence) . . . . .	53
4.19 Longitudinal distribution, narrow spacing, laminated guide, $f=17.0$ GHz (probe centered)	54
4.20 Longitudinal distribution, narrow spacing, laminated guide, $f=17.0$ GHz (probe next to fence) . . . . .	55
4.21 Comparative mode distribution, wide, empty and narrow, empty . . . . .	56
4.22 Comparative mode distribution, wide, empty and wide, $2x1/16$ . . . . .	57
4.23 Comparative mode distribution, wide, empty and wide, round . . . . .	58
4.24 Comparative mode distribution, wide, empty and wide, laminated . . . . .	59
4.25 Comparative mode distribution, narrow, empty and narrow, $2x1/16$ . . . . .	60
4.26 Comparative mode distribution, narrow, empty and narrow, round . . . . .	61
4.27 Comparative mode distribution, narrow, empty and narrow, laminated . . . . .	62
4.28 Q-value measurements of guide, wide and narrow spacing, with no inserts . . . . .	63
4.29 Q-value measurements of guide, wide and narrow spacing, with no inserts . . . . .	64
4.30 Q-value measurements for guide, wide spacing, with three insert configurations, empty, $2x1/16$ , and laminated . . . . .	65
4.31 Q-value measurements for guide, wide spacing, with three insert configurations, empty, $2x1/16$ , and laminated . . . . .	66

## LIST OF FIGURES (continued)

## Page

4.32 Q-value measurements for guide, narrow spacing, with three insert configurations, empty, 2x1/16, and laminated . . . . .	67
4.33 Q-value measurements for guide, narrow spacing, with three insert configurations, empty, 2x1/16, and laminated . . . . .	68
4.34 Q-value measurements of guide, wide spacing with half-round inserts at two frequencies .	69
4.35 Q-value measurements of guide, narrow spacing, with half round inserts at two frequencies . . . . .	70
4.36 Leakage, wide guide, empty . . . . .	73



## 1. INTRODUCTION

There are considerable difficulties encountered in the transmission of millimeter waves. Due to high attenuation and low power handling capabilities of conventional rectangular waveguides at millimeter wave frequencies it has become necessary to investigate the properties of non-conventional waveguide structures. The fence guide is one such non-conventional structure that seems to offer improvements over the conventional guides. The fence guide is an H-type structure which offers simple fabrication and use of the H-guide structure offers improvements such as reduced attenuation.

Investigation of the fence guide was carried out at 35 GHz. This investigation deals with the properties of the fence guide at a lower frequency (12-18 GHz.) where some of the problems encountered in the previous measurements could be eliminated. This investigation was also concerned with the fence-guide characteristics when the guide was loaded with additional dielectrics.

## 2. LITERATURE SURVEY

### 2.1 Introduction

The concept of fence guides finds its origin in H-guides and reactive-wall waveguides. An H-guide is an open type waveguide, with a cross-sectional form of an H. The H-guide essentially consists of two parallel conducting plates separated by a dielectric strip. Apart from being a simple structure, H-guides have the property that the attenuation decreases with increasing frequency. A fence guide is an H-guide with the parallel conducting plates replaced by reactive wire grids (fence). The possibility of simplified fabrication and design of circuitry at high frequencies prompted further investigations of the fence guide structures.

### 2.2 H-Guide

Tischer (1953) proposed the H-guide and later its theory of operation including the computation of surrounding fields. From this work he found that the attenuation, lower than in rectangular or circular waveguides, decreased continuously with increasing frequency. Further study by Tischer (1956) showed that the cross-sectional distribution of the density of the energy flow can be manipulated, within certain limits, by proper dimensioning of the H-guide. In still

further work, Tischer (1958) investigated, both theoretically and experimentally, wave propagation in modified H-guides, in laminated H-guides, and in groove guides at both X-band and in millimeter bands. He specifically considered losses due to radiation, conduction, and dielectric.

In 1959, Griemsmann and Birenbaum experimenting with H-guides and a foam dielectric (dielectric constant 1.03), reported an attenuation of 1.05 dB/meter at a frequency of 50 GHz. They also proposed some preliminary configurations for components and instruments for H-guides including: bends, couplers, and standing wave detectors. Tischer (1959) also conducted experimental investigations of H-guides and a laminated-dielectric guide, and in 1969 he presented a more general treatment of this type of guide. In this treatment he found that by using a laminated dielectric, dielectric losses could be further reduced. By reducing the dielectric losses attenuation is made less.

### 2.3 Wire Grids

In recent years Macfarlane (1946) studied impedance properties of infinite plane grids of parallel equidistant circular wires. He considered the radius of the wire to be much smaller than the wire spacing. Lewis and Casey (1952), in analysing gratings of



resistive wires, studied the effect of resistivity on reflection and transmission. Wait (1954) studied the problem, of parallel wire grids for a plane wave incident obliquely with arbitrary polarization, using quasi-stationary methods.

All the studies of the fences were made using the assumption that the radius of the wire was much less than the spacing. Investigation of the properties of silver plated grids and brass wire grids were made by Duncan and Tischer (1968) for moderately spaced grids at X-band. For dense wire grids, as used in fence guides, the above treatment yields erroneous and unrealistic results. Further studies of the characteristics of dense wire grids were made by Tischer (1970) and a modified surface impedance formula was proposed.

#### 2.4 Fence Guide

The fence guide, originally proposed by Tischer (1968), is a reactive-wall waveguide in the H-guide configuration. The mode analysis and field distribution was studied using the direct field approach. Fences of metallic strips were also considered, however, because of ease of fabrication wire grids were

---

Duncan & Tischer, Progress Report Grant NGR  
34-002-047/S1 October 15, 1968. N.C.State  
University.

Tischer, Progress Report Grant NGL 34-002-047 June 15,  
1970. N.C.State University.

preferred. The analysis of the fence guide was expanded by Tischer (1968), to include the losses in the reactive walls. In this analysis, attenuation and phase factors were derived. Preliminary measurements were made to verify the theoretical computations and relatively high values of attenuation were observed. By lowering the propagation constant  $k_z$ , attempts were made to reduce guide losses through dielectric loading.

An experimental study of the field distribution about the fence guide was made by Kraft and Summerlin (1970). This study was made at a frequency of 35 GHz and included an analysis of several types of measurement probes. Further field measurements and comparative studies were carried out by Agarwal and Tischer (1970) on fence guides with slightly different post spacings. They also studied the effects of dielectric loading on the Q-value of the fence guide resonators.

Tischer, 1968. Progress Report Grant NGR  
34-002-47/S1 July 30, 1968. N.C.State  
University.

Tischer, 1968. Progress Report Grant NGR  
34-002-047/S1 October 15, 1968. N.C. State  
University.

Kraft & Summerlin. Progress Report Grant NGL  
34-002-047 February 15, 1970. N.C. State  
University.

Agarwal & Tischer. Progress Reports Grant NGL  
34-002-047 June 15, 1970 and October 15, 1970.  
N.C.State University.

### 3. EXPERIMENTAL MEASUREMENT TECHNIQUES

#### 3.1 Introduction

An experimental study of the fence guide was carried out in the  $K_u$ -Band (12-18 GHz.) frequency range for several reasons: (1) ease of prototype fabrication, (2) increased measurement accuracy, and (3) better probe-to-wavelength ratio.

With the manufacturing facilities available, fabrication of fence guides for high frequencies was a problem. Kraft (1970) encountered these problems when designing a prototype section of the fence guide for measurements at 35 GHz. He found that for the separation of wires to be used, the drilling of the post holes in the dielectric caused the dielectric to become fragile. He also found that post alignment was difficult to obtain.

Another reason was the fact that measurement accuracy in general increases at lower frequency because of more developed, readily available measurement equipment.

The greatest advantage of a lower frequency is the probe size. The ratio of probe size to wavelength can be made much smaller. This causes much less field distortion and thus more representative measurements of the fields. Even at  $K_u$ -Band frequencies probe

loading was a problem. If the probe was inserted too far into the fence guide, distortion due to probe loading was appreciable. Probe loading was least noticeable when the probe was inserted close to the fence.

### 3.2 Waveguide

#### 3.2.1 Fence guide

The fence guide basically represents a reactive-wall H-guide. The customary conducting walls forming the sides are replaced by wire grids which can be considered reactive-walls. The basic field distribution in an H-guide type structure is described by the following equations (see Figure 3.2).

In dielectric:

$$E_x^\epsilon = \frac{E_{x0}^\epsilon k_z h}{\epsilon_r k_x} \cos(k_x x) \cos(k_y y) e^{-jk_z z},$$

$$E_y^\epsilon = \frac{E_{y0}^\epsilon k_y k_z h}{\epsilon_r (k_y^2 + k_z^2)} \sin(k_x x) \sin(k_y y) e^{-jk_z z},$$

$$E_z^\epsilon = \frac{E_{z0}^\epsilon j k_z^2 h}{\epsilon_r (k_y^2 + k_z^2)} \sin(k_x x) \cos(k_y y) e^{-jk_z z},$$

$$H_y^\epsilon = \frac{H_{y0}^\epsilon \omega \epsilon_0 k_z^2 h}{k_x (k_y^2 + k_z^2)} \cos(k_x x) \cos(k_y y) e^{-jk_z z},$$

and

$$H_z^\epsilon = \frac{H_{z0}^\epsilon j \omega \epsilon_0 k_y k_z h}{k_x (k_y^2 + k_z^2)} \cos(k_x x) \sin(k_y y) e^{-jk_z z}.$$



In air:

$$E_x^a = E_{x0}^a k_z e^{-\alpha_x x} \cos(k_y y) e^{-jk_z z},$$

$$E_y^a = \frac{E_{y0}^a \alpha_x k_y k_z}{(k_y^2 + k_z^2)} e^{-\alpha_x x} \sin(k_y y) e^{-jk_z z},$$

$$E_z^a = \frac{jE_{z0}^a \alpha_x k_z^2}{(k_y^2 + k_z^2)} e^{-\alpha_x x} \cos(k_y y) e^{-jk_z z},$$

$$H_y^a = \frac{H_{y0}^a \omega \epsilon_0 k_z^2}{(k_y^2 + k_z^2)} e^{-\alpha_x x} \cos(k_y y) e^{-jk_z z},$$

$$H_z^a = \frac{jH_{z0}^a \omega \epsilon_0 k_y k_z}{(k_y^2 + k_z^2)} e^{-\alpha_x x} \sin(k_y y) e^{-jk_z z}.$$

The basic structure is illustrated in Figure 3.1. The physical size of the fence guide makes operation below 12 GHz (cutoff frequency), excepting special applications, impractical. (See section 3.2.2 for dimensions, smaller dimensions imply a higher cutoff frequency.)

### 3.2.2 Actual Prototype

The actual fence guide section (Figure 3.3) is built on a piece of dielectric (1422 Rexolite, American Enka Corp.) with walls of the guide made of parallel rows of silver plated brass posts. Photographs of the actual measurement setup and closeups of the prototype section are shown in Figure 3.4 to 3.8. Two fence guide prototypes were fabricated for this experiment. They are identical except for the center to center spacing of the posts. The center to center spacing of one section was twice



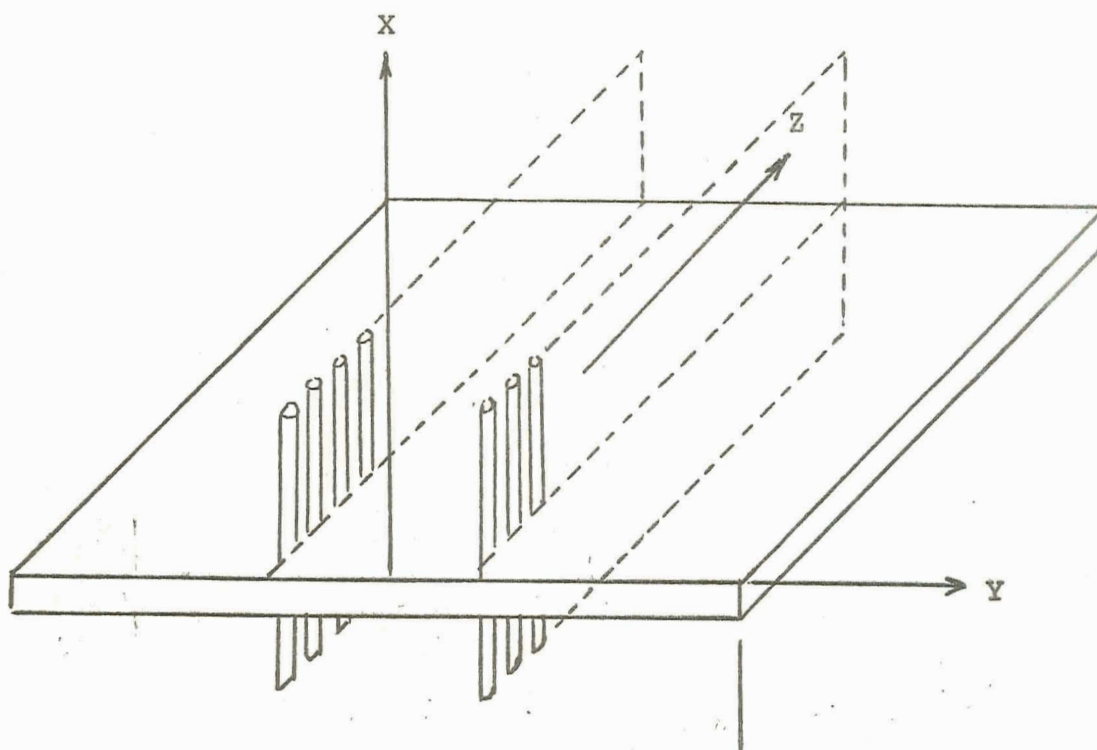


Figure 3.1 Basic fenceguide and coordinate system.

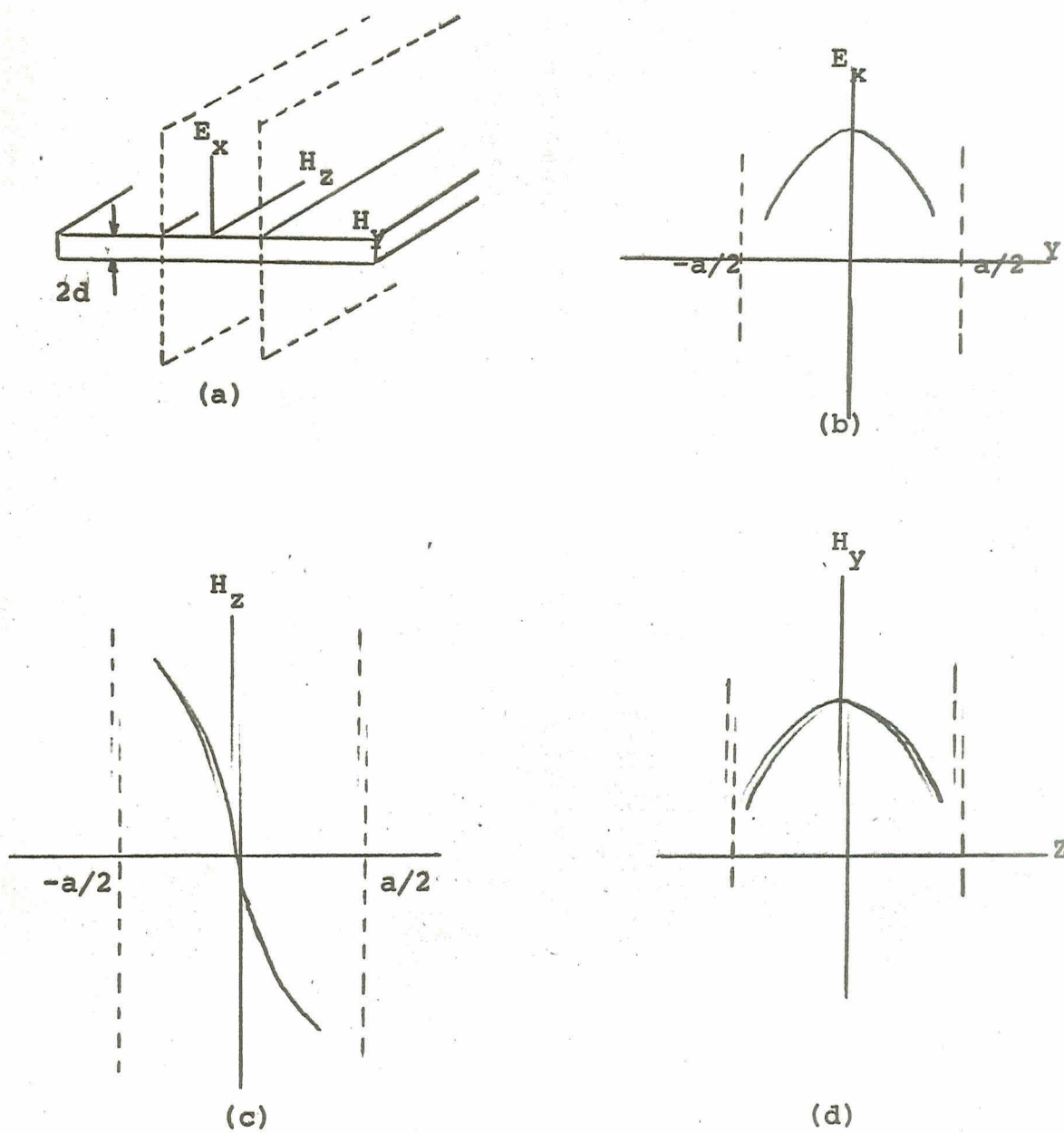


Figure 3.2 Field distribution in fence guide.

(a) Field components.

(b)  $E_x$ .

(c)  $H_z$ .

(d)  $H_y$ .

dimensions in cm unless otherwise indicated

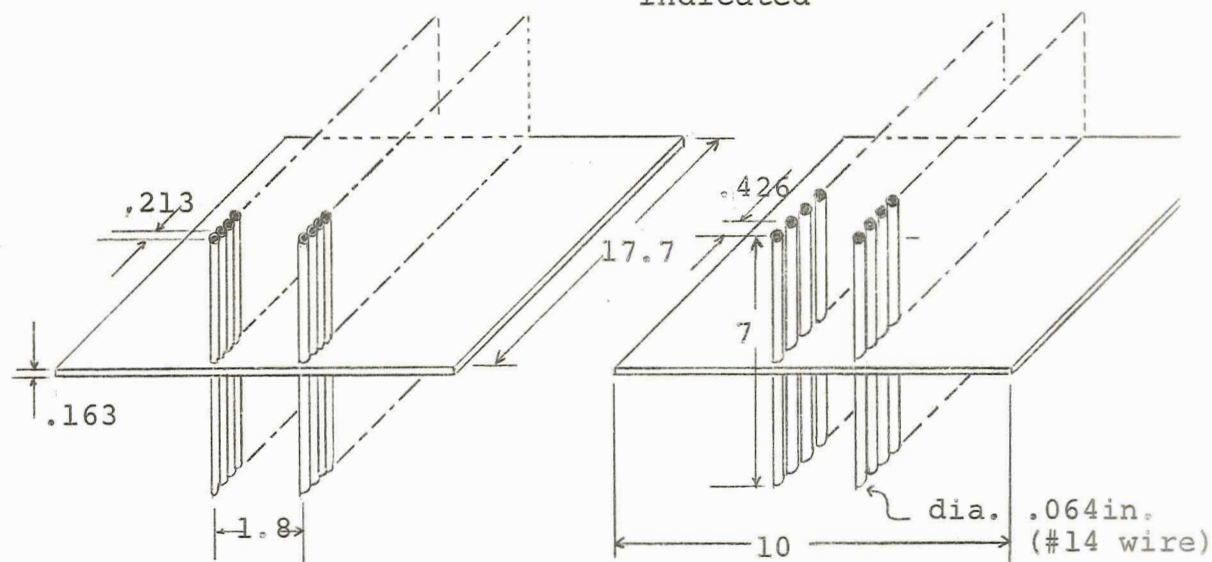


Figure 3.3 Dimensions of prototype guide. (Note that dimensions of both guides are identical except for post spacing)

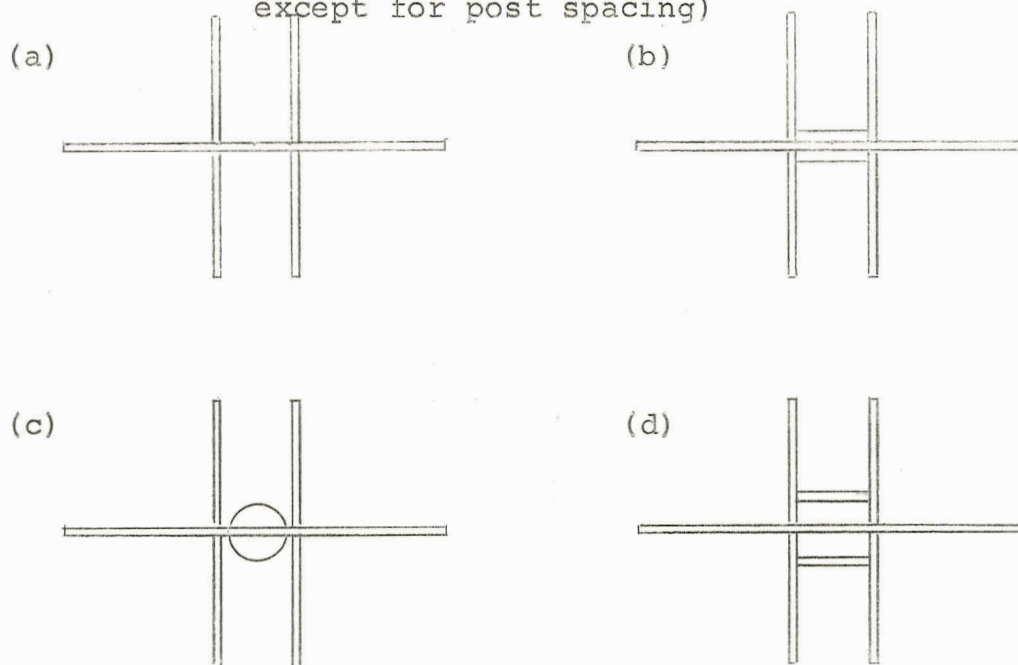


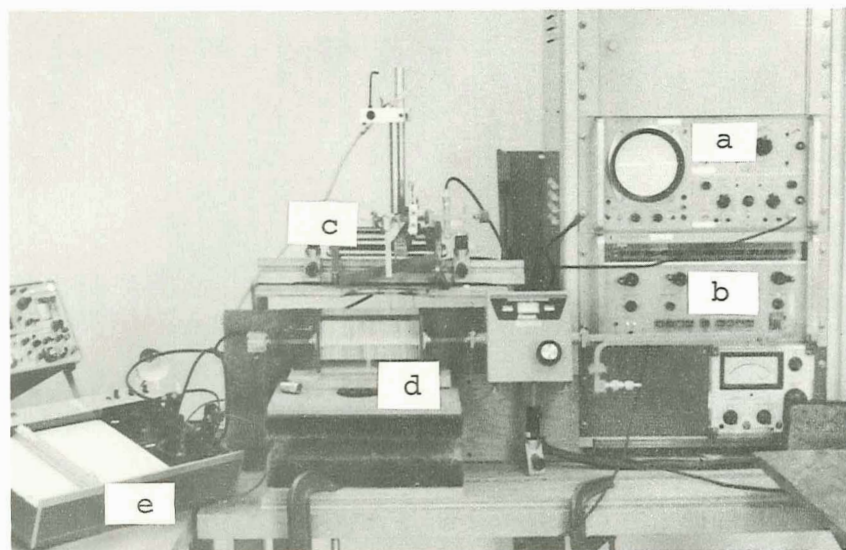
Figure 3.3A Cross sections of tested guide  
 (a) basic fence guide (c) central dielectric loading  
 (b) 2x1/16 dielectric loading (d) laminated guide

that of the other section. See Figure 3.3 for the exact dimensions.

The characteristics of each guide were observed with several different dielectric insert configurations. See Figure 3.3A for description of physical dimensions of the inserts. These inserts were placed on both sides of the center dielectric slab to determine their effects on the fields. It has been shown theoretically, Tischer (1970), that the exponential decay in the x direction should increase with dielectric loading. Three types of inserts were used for loading and the measurements were compared to the empty guide section.

The fence-guide configurations used were as follows: (1) guide with widely spaced posts, no inserts, (2) guide with closely spaced posts, no inserts, (3) guide with widely spaced posts and 1/16" dielectric inserts on each side of main dielectric, (4) guide with closely spaced posts and 1/16" dielectric inserts on each side of main dielectric, (5) widely, and (6) closely spaced posts with half round dielectric inserts on each side of main dielectric, (7) widely, and (8) closely spaced posts with laminations. These configurations will hereafter be empty, (3) wide 2x1/16, (4) narrow 2x1/16, (5) wide round, (6) narrow round, (7) wide laminated, and (8) narrow laminated.





- a. 'O' Scope
- b. Sweep generator
- c. Sliding probe carriage
- d. Prototype guide

- e. Plotter
- f. Probe

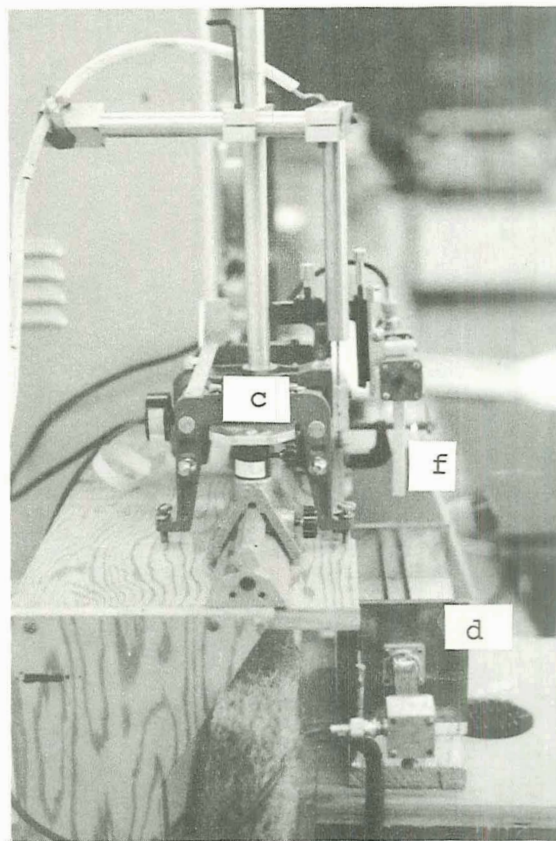
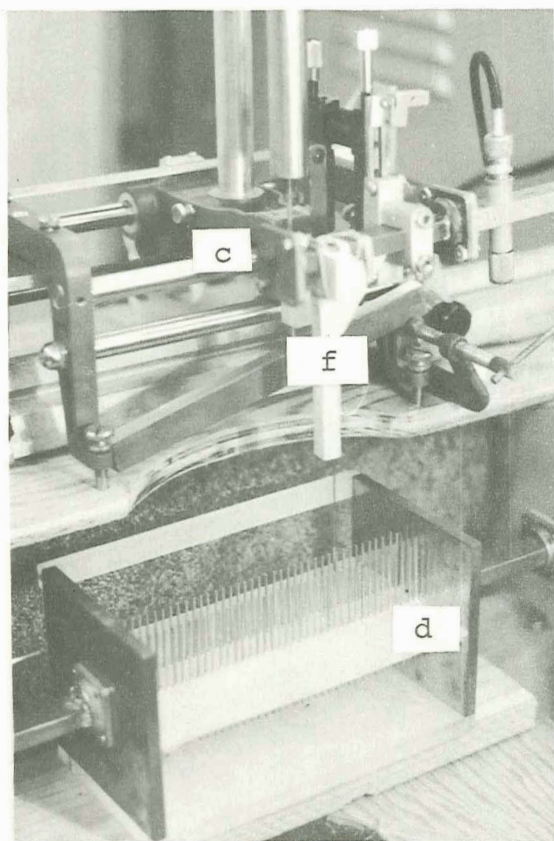


Figure 3.4 General purpose measurement setup





Figure 3.5 Prototype guide, narrow spacing.

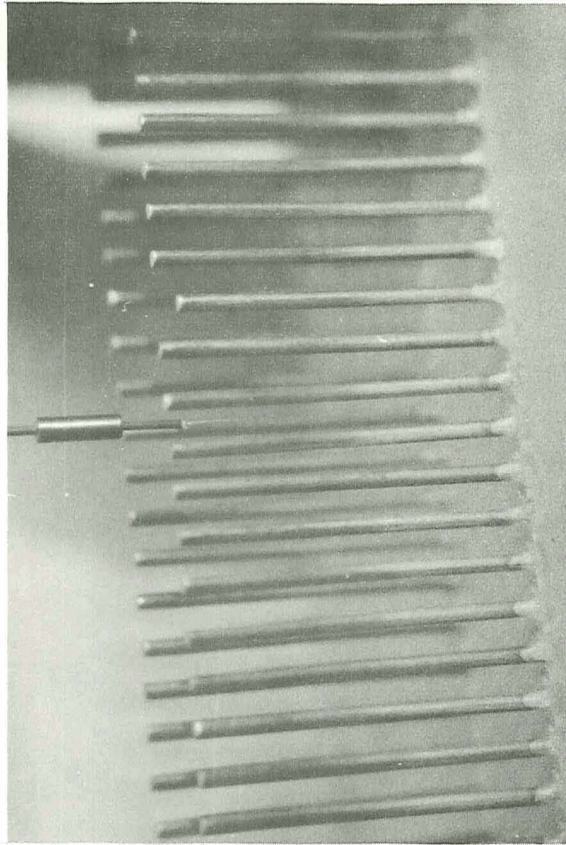


Figure 3.6 Prototype guide, wide spacing with probe

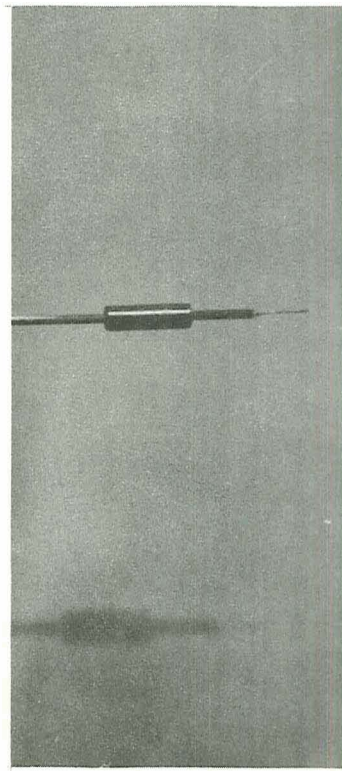


Figure 3.7 Compensated-dipole probe. (see sec.

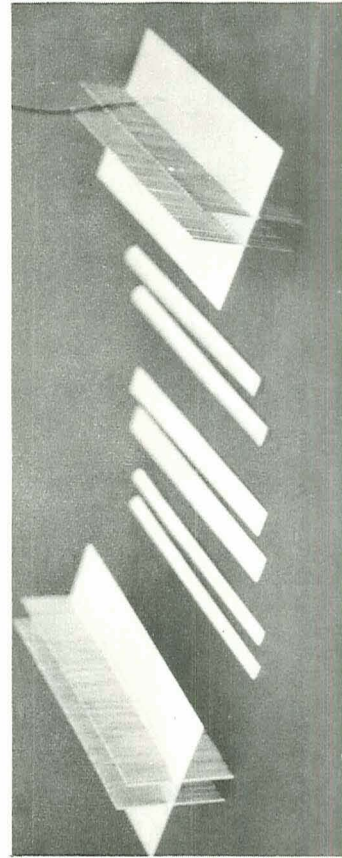


Figure 3.8 Prototype guides with dielectric inserts. (See fig.

### 3.3 Description of Equipment

#### 3.3.1 General Test Equipment

A Hewlett Packard signal sweep generator provided a leveled sweep from 12.5-18 GHz. The sweep generator also provided the signal that was convenient for Q-value measurements and a CW output, either modulated or unmodulated for field distribution measurements. A Hewlett Packard oscilloscope was used as a monitor for the Q-value and mode distribution measurements and an X-Y Plotter was employed to make a permanent record of all the measurements. Detailed schematics for different measurement setups will be given in the following sections.

#### 3.3.2 Special Equipment

##### 3.3.2.1 The Probe

For accurate measurements of the field intensity distribution, the following requirements were made for the probe:

1. Any distortion of the fields by the probe must not seriously affect the accuracy of the measurements.

2. Physical features of the probe must be small enough to essentially measure the field at a point.

The type of probe selected for measurements in the fence-guide described earlier was the capacitive compensated dipole. Results of Kraft and Summerlin (1970), show that the capacitive dipole is better suited for these

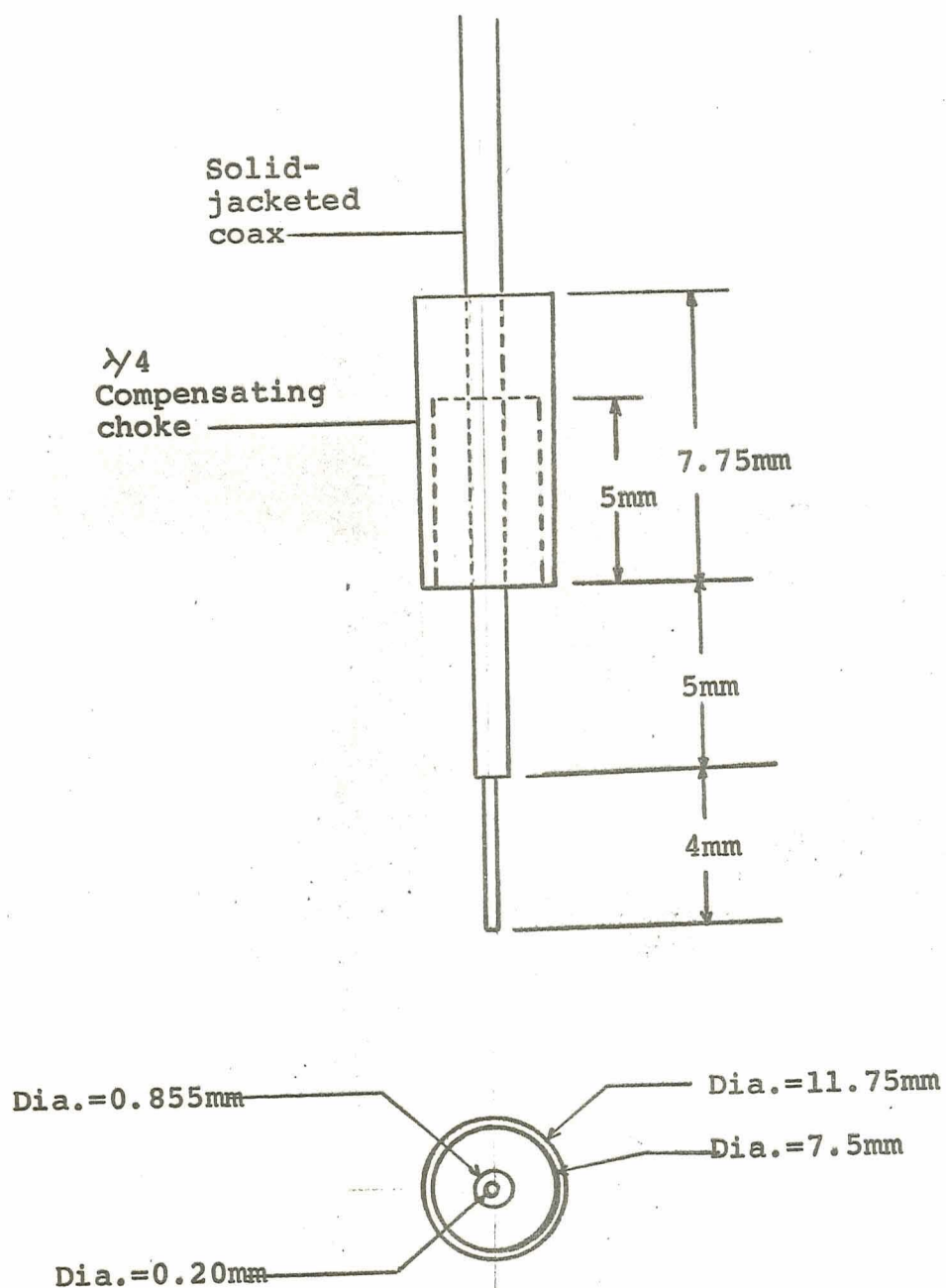


Figure 3.9 Probe dimensions (Scale 5:1)



measurements than the other probes available. The probe dimensions are given in Figure 3.9, and a closeup photograph is shown in Figure 3.7.

The probe is constructed of miniature solid-jacketed coaxial cable, with an outer conductor of copper, diameter 0.85 mm, and an inner conductor of silver, diameter 0.20 mm. The outer conductor is stripped 4.0 mm exposing the inner conductor. The outer conductor extends into a quarter wavelength choke, which acts as an infinite impedance to waves traveling up the feed line.

The individual probe characteristics are determined by plotting the relative field intensity in front of an open rectangular waveguide. (See Figures 3.10 to 3.13). Figures 3.10 and 3.12 show probe leakage with the choke and Figures 3.11 and 3.13 show probe leakage without the choke at the frequencies indicated. With the choke, the leakage is 15 dB down from the maximum at 13.4 GHz. and without the choke the leakage is only 3 dB down. For 17 GHz. with the choke, leakage is 8-10 dB down and without the choke leakage is only 3-4 dB down. These measurements were taken after the choke had been positioned to give the least leakage in the middle of the band, at 15 GHz. A quarter wave choke was used for the 15 GHz range.



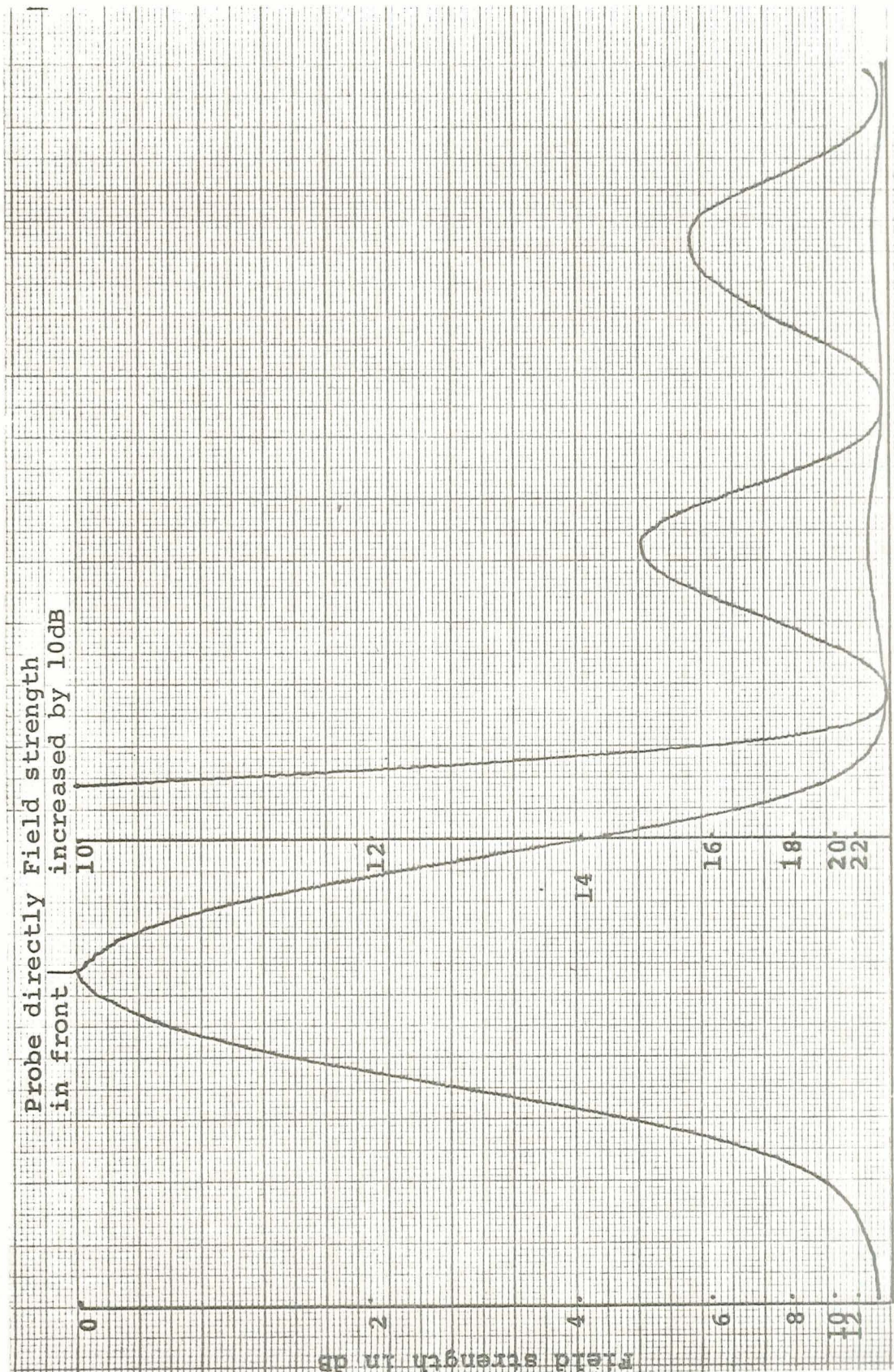


Figure 3.10 Probe with compensation cavity in front of open guide at 13.4GHz.



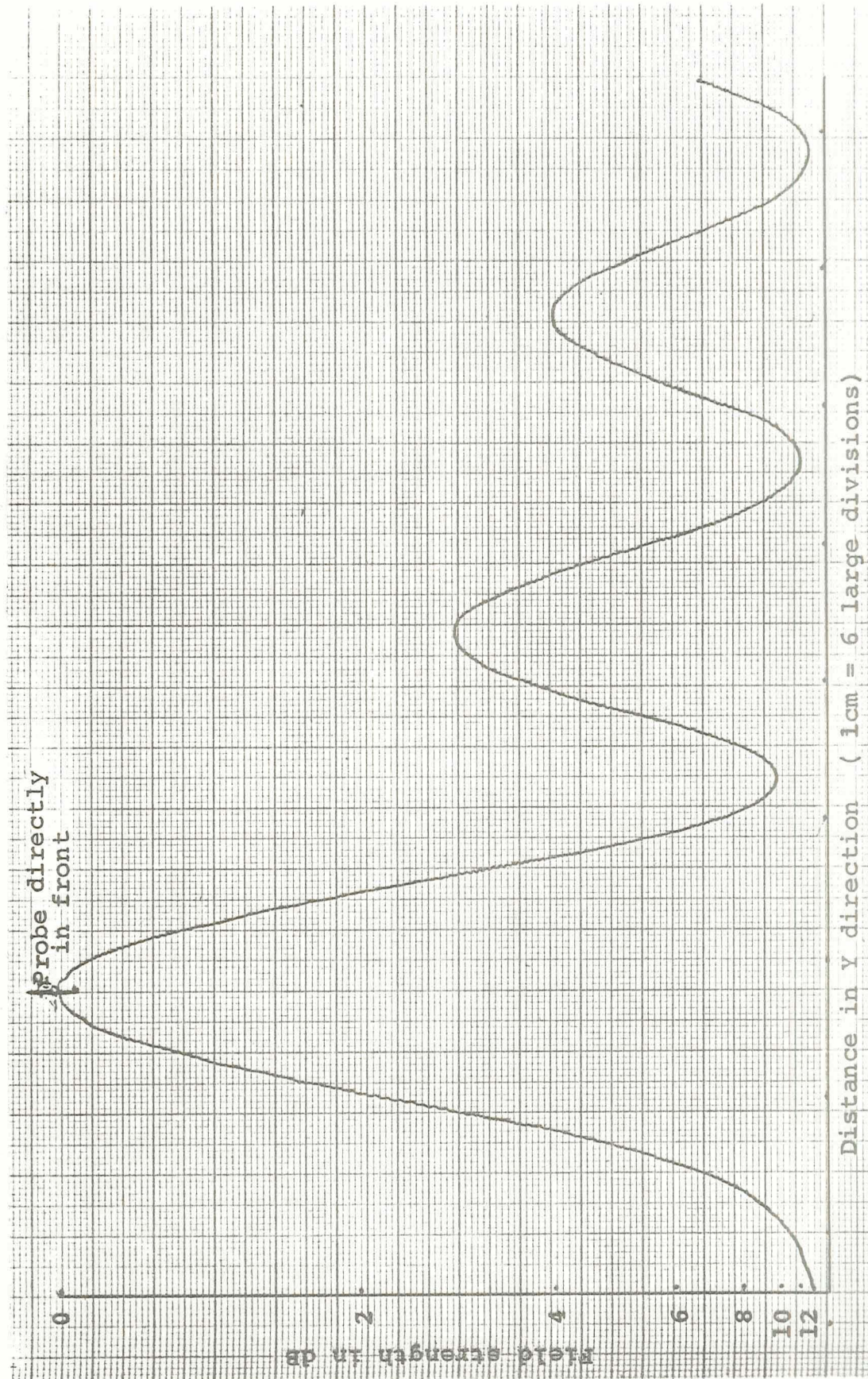


Figure 3.11 Probe without compensation cavity in front of open guide at 13.4GHz 19



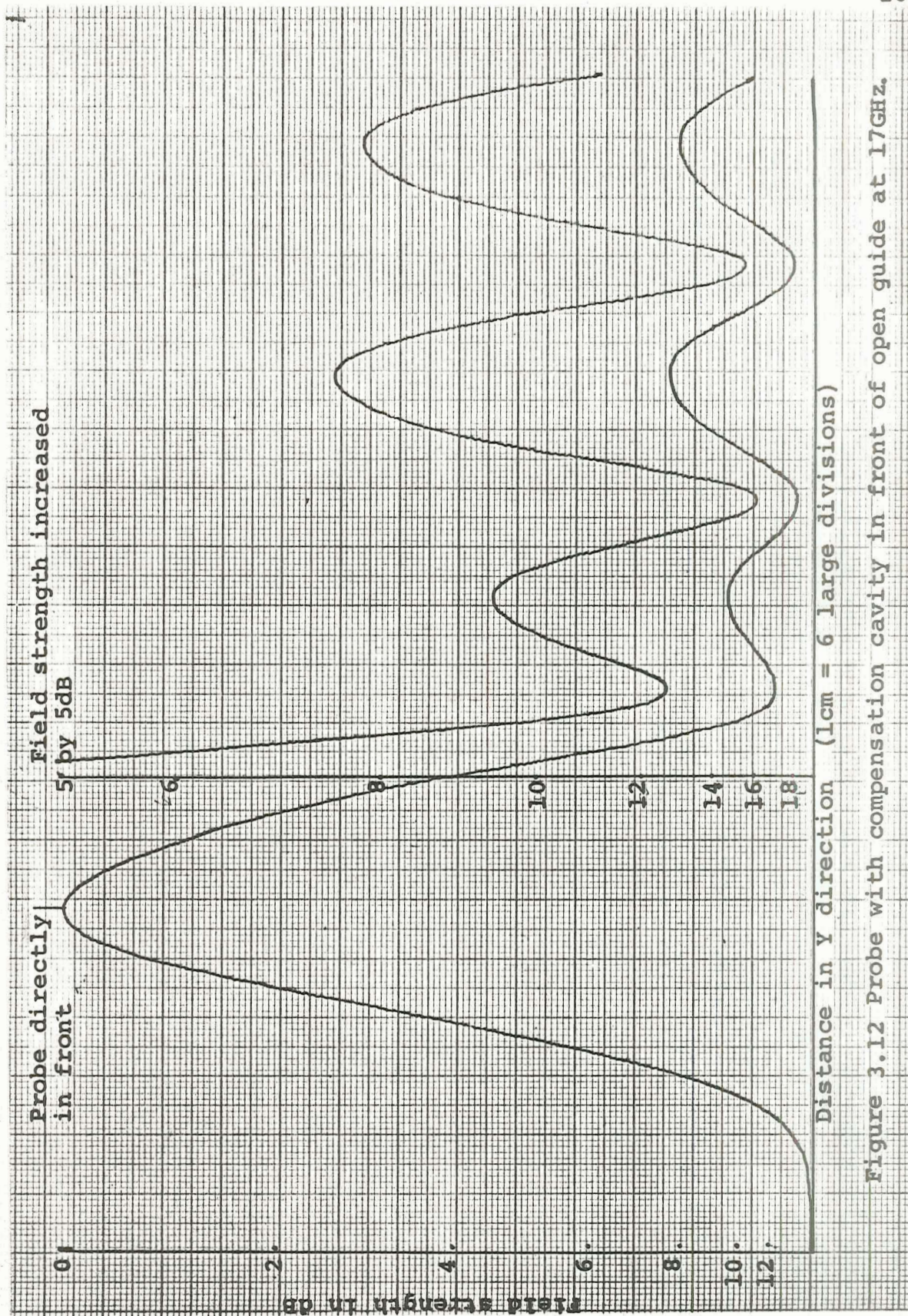
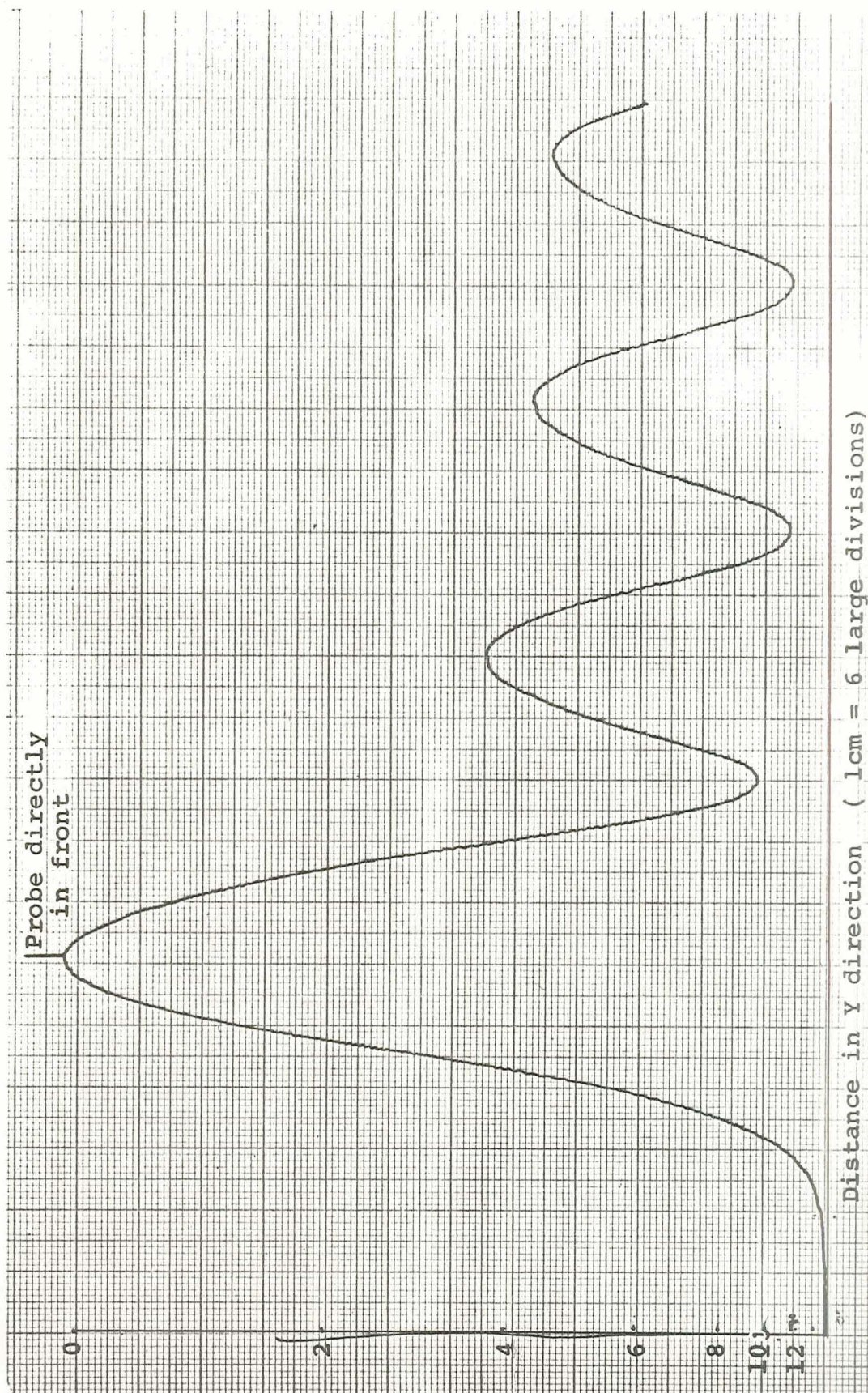


Figure 3.12 Probe with compensation cavity in front of open guide at 17GHz.





Distance in Y direction (1cm = 6 large divisions)

Figure 3.13 Probe without compensation cavity in front of open guide at 17GHz



### 3.3.2.2 Graphing Equipment and Techniques

By the use of a linear transformer type 60 Hz function generator it was possible to use the plotter for field measurements. The transformer which has a cylindrical form, has a rod which moves along the transformer axis. The output voltage of the transformer is a linear function of the position of the rod. By construction of an appropriate holder, the transformer, a cylinder 7" long and 1" in diameter with a core (rod) positioned along the longitudinal axis, can be used to represent probe movement in either the X,Y, or Z direction, see Figure 3.1. The linear range for the transformer is 2". This range was extended to 10 cm for measurements in the Z direction by the use of an inclined plane.

### 3.4 Q-Value Measurement Techniques

A swept-frequency method was used to facilitate measurements with continuous recording of data. The swept-frequency generator is connected to the input of the prototype fence-guide section through a precision attenuator. The output signal is measured at the exit port of the section. The input signal is essentially independent of frequency due to the signal leveling system of the sweep oscillator. The sweeping range  $\Delta f$  was equal to 50 MHz. The circuit is shown in Figure 3.14. For some selected mode the desired frequency range was set and the precision attenuator was adjusted to some integer setting. With the output of the cavity connected

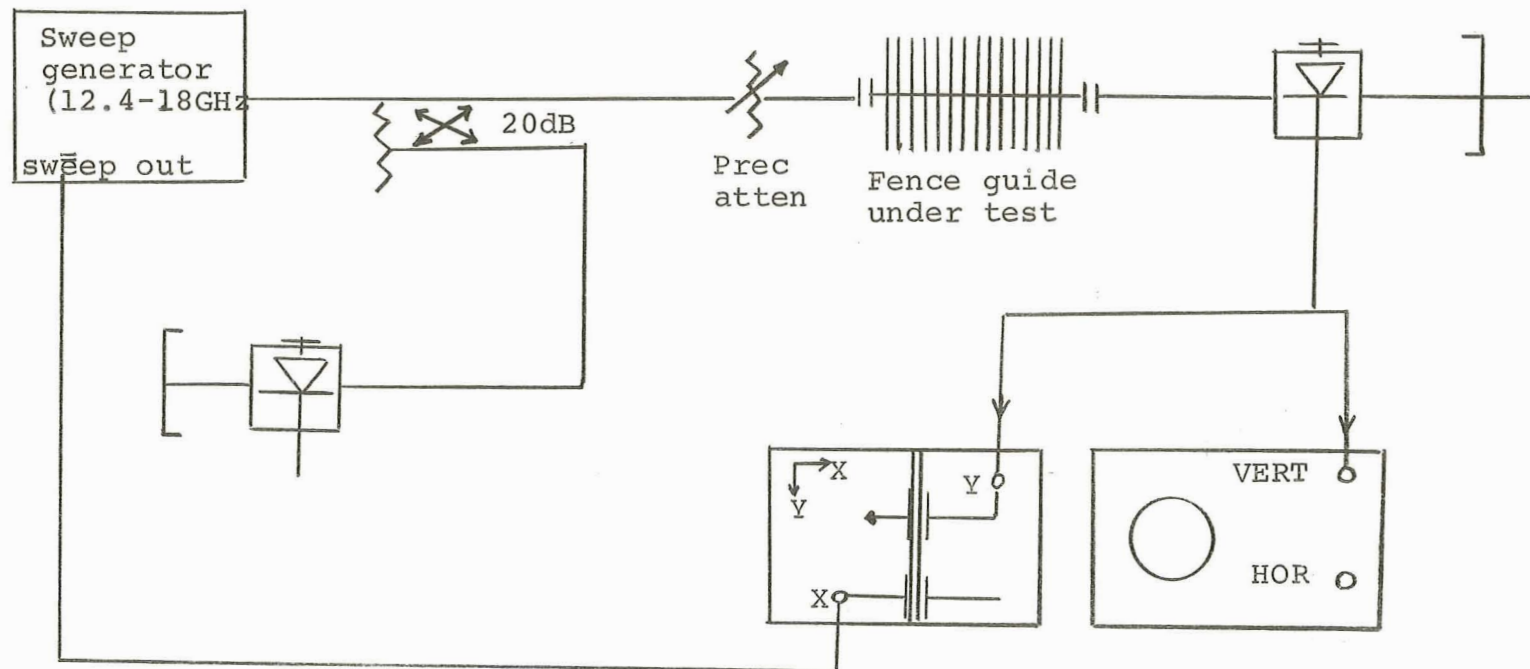


Figure 3.14 Test-bench setup for Q value and mode-distribution measurements. 23



to the vertical input of the plotter, and with the same sawtooth signal that was sweeping the oscillator connected to the horizontal input of the plotter, the Q-curve was traced. Then additional 3 dB of attenuation was inserted by adjusting the attenuator, and another Q-curve was traced. A horizontal line across the peak of the second curve intersects the first curve at the 3 dB points. These 3 dB points represent the half power frequencies of the mode. As the Q-values for the fence-guide section are relatively high, the following equation will be used to compute Q-values

$$Q = \frac{f_o}{\Delta f} ,$$

where  $f_o$  is the resonant frequency of the mode and  $\Delta f$  is the frequency difference between the half power frequencies.

### 3.5 Mode Distribution Measurements

The same measurement setup was used as that for Q-value measurements except that the sweep frequency was over the whole band from 12.5-18 GHz. The plotter was connected in the same way. During plotting, the sweeping speed was adjusted to 100 seconds per sweep to allow ample time for the plotter to follow the sharp Q modes. After the complete mode distribution was plotted the resonant frequencies of each mode were checked and recorded. Mode frequencies were measured with the cavity type frequency meter.



### 3.6 Field Measurements

With the probe inserted into the fence-guide for the longitudinal field distribution measurements the probe carriage was moved in the Z direction. Figure 3.4 shows the arrangement. The probe output was coupled into a rectangular waveguide and, with the waveguide thus excited, this output was detected by a crystal detector, and sent to the oscilloscope and the vertical input of the plotter. The horizontal input for the plotter was taken from the linear transformer which has been described previously. By adjusting the horizontal gain of the plotter the longitudinal distance was calibrated for a desired scaling factor on the graphs.

## 4. MEASUREMENTS

### 4.1 Introduction

From the data obtained by the measurements the following characteristic parameters were derived:

$k_z$ ,  $\beta_z$ ,  $\lambda_g$ ,  $\alpha_z$ ,  $k_y$ , and  $\alpha_x$  where

$k_z$  = longitudinal propagation constant,

$\beta_z$  = longitudinal phase constant

$\lambda_g$  = guide wavelength,

$\alpha_z$  = longitudinal attenuation factor,

$k_y$  = transverse propagation constant (y dir.),

and  $\alpha_x$  = transverse attenuation factor (x dir.).

Secondary effects were also observed, such as yagi-waves (wave forms typical for the wave propagation on yagi antennas present when round dielectric inserts were used), and probe loading.

The measurements consisted of 3 basic types:

1) longitudinal distribution,

2) frequency distribution of modes,

and 3) Q-value.

Other observations such as field intensity ratios of the value inside to the value outside of the fence, and the effects of absorption material on yagi-waves were also made.



## 4.2 Longitudinal Characteristics

### 4.2.1 Introduction

From an analysis of the measured Q-values, mode and longitudinal distribution measurements, the longitudinal field parameters ( $\alpha_z$ ,  $\beta_z$ ,  $\lambda_g$ , and  $k_z$ ) were found. The values of  $\lambda_g$  were determined directly from the diagrams of the longitudinal field distribution, Figure 4.6 to 4.20 and also from the mode distribution curves, Figure 4.21 to 4.27 (see section 3.5). By using these values of  $\lambda_g$  and the relationship

$$\beta_z = \frac{2\pi}{\lambda_g} ,$$

the phase constant  $\beta_z$  was evaluated. The method used for obtaining  $\alpha_z$  is based on the relationship between  $\alpha_z$  and the Q-values. The method will be discussed later.

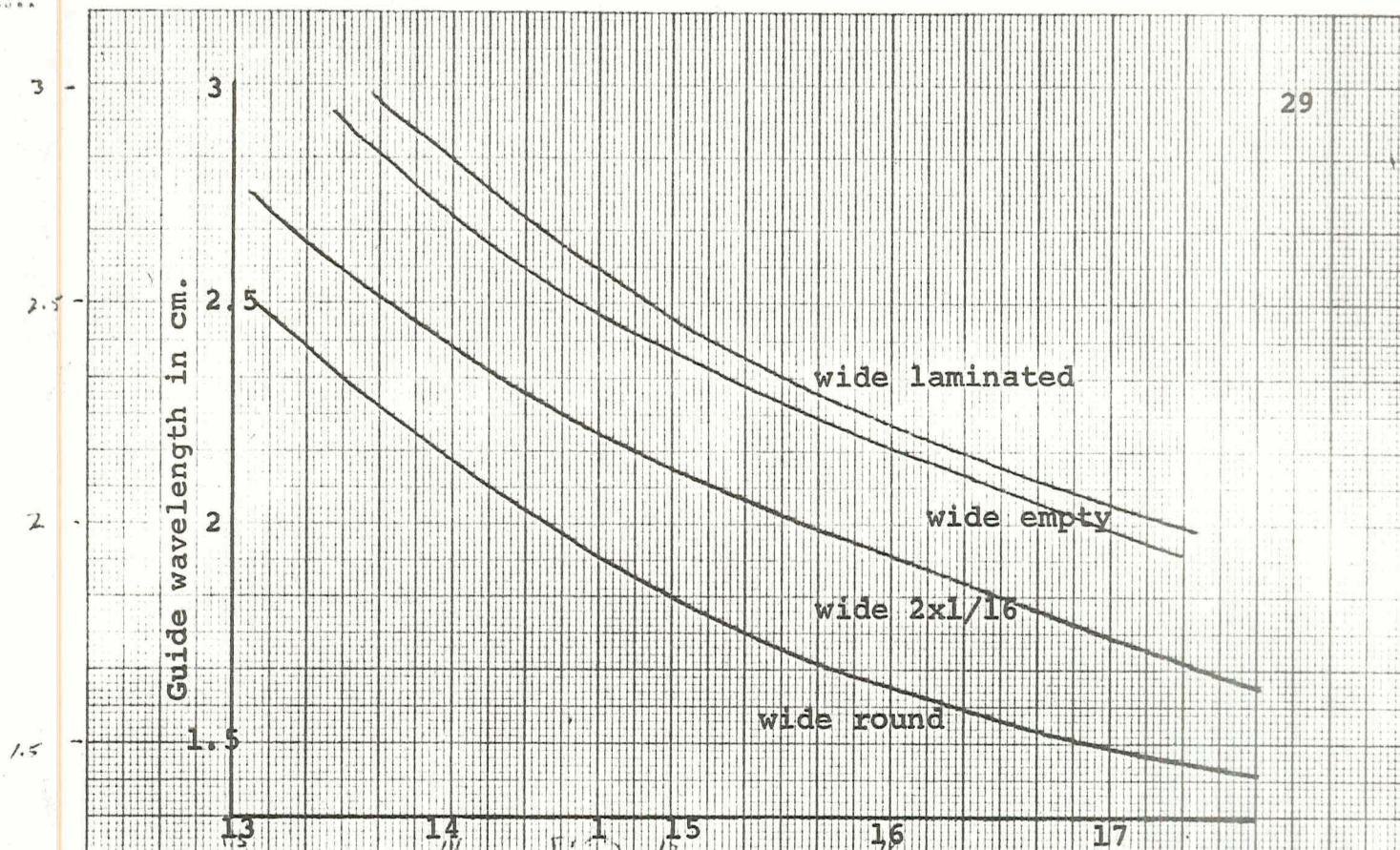
### 4.2.2 Determination of $\lambda_g$

By counting the number of maxima for the entire length of the guide for a particular resonant mode the value of  $\lambda_g$  can be determined by the following equation:

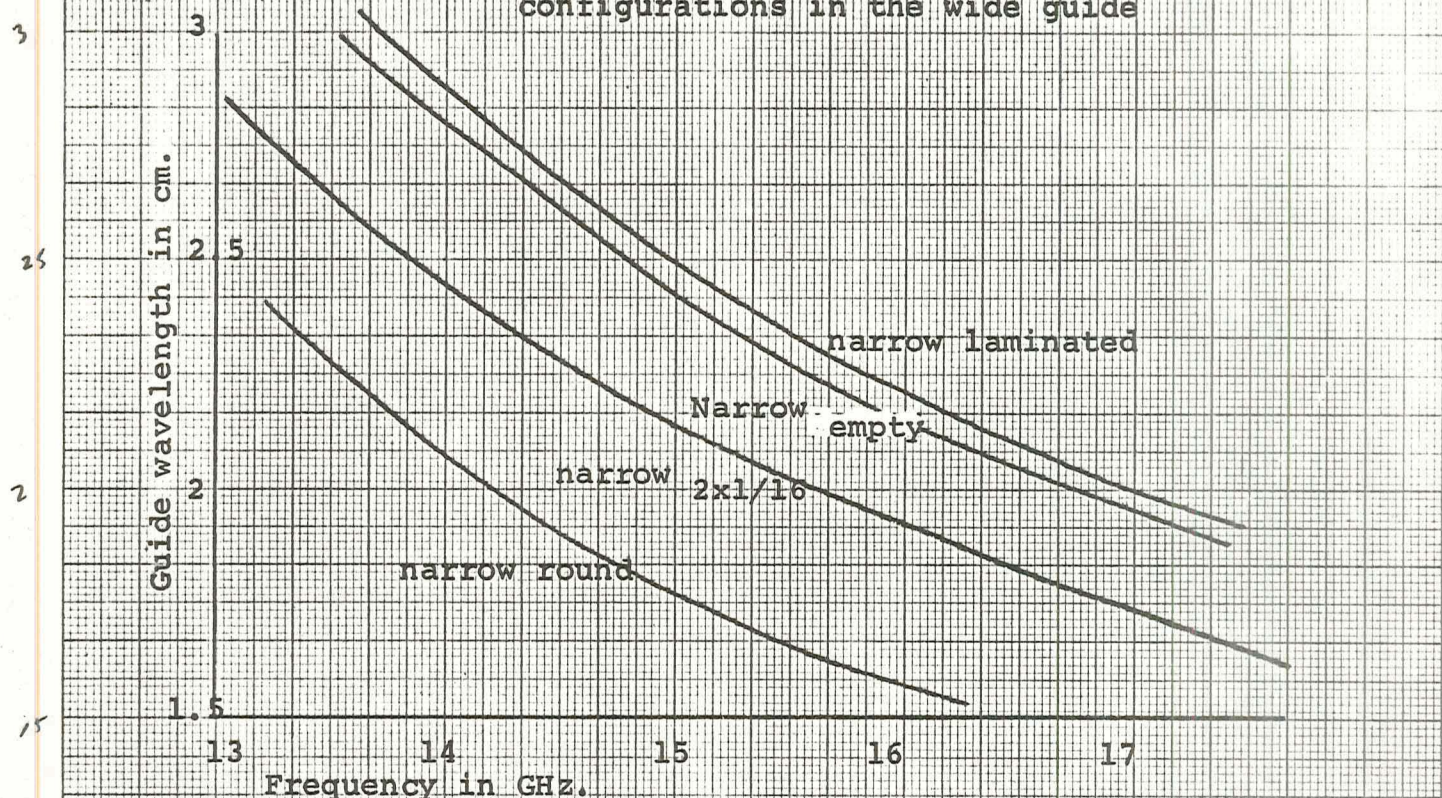
$$\lambda_g = \frac{2(\text{length of shorted section of guide})}{\text{number of half period variations}} .$$

Guide wavelength,  $\lambda_g$  may also be measured directly from Figures 4.6 to 4.20, with the knowledge of the scale factor (2 cm on graph equal 1 cm). Figures 4.1 and 4.2 illustrate the relationship between guide wavelength and frequency for the various configurations.





Frequency in GHz.  
Figure 4.1 Guide wavelength vs. frequency for various configurations in the wide guide



Frequency in GHz.  
Figure 4.2 Guide wavelength vs. frequency for the various configurations in the narrow guide.



#### 4.2.3 Relationship of Q-value and $\alpha_g$

A direct measurement of attenuation can be accomplished by measuring the power change per unit length. The power change can be measured by probes inserted into a section of guide. The probe, however, distorts the field and introduces errors. Measurements of the Q-value of a shorted section of waveguide are not hampered by these difficulties. For this reason this method was used. The Q-value can be related simply to attenuation. Equations for this purpose were developed for H-guide by Adair (1970). The relationship will be used as an approximation for fence-guides. The equation is

$$\alpha_z = \frac{k_o^2 C}{2k_z Q} \quad , \quad (4.1)$$

where

$$k_o = 2\pi / \lambda_o \quad ,$$

$$k_z = 2\pi / \lambda_g \quad ;$$

and

C is a correction factor given by

$$C = \frac{k_x + \frac{\alpha_x}{k_x} (\epsilon_r \alpha_x + h^2 d)}{k_x + \frac{\alpha_x}{\epsilon_r k_x} (\epsilon_r \alpha_x + h^2 d)} \quad .$$

Diagrams for these equations are available and were used for the evaluation.

---

Adair & Tischer, Progress Report Grant NGL 34-002-047  
February 15, 1970. N.C.State University.

#### 4.2.4 Evaluation of $\alpha_z$

To use the information given in section 4.2.3, the factors of equation 4.1 must be defined for each one of the configurations (Figure 3.3). Table 4.3 gives the Q-values available for certain modes of each configuration. Figure 4.3 gives the correction factor C for the dielectric used ( $\epsilon_r = 2.53$ ) as a function of  $d/\lambda_0$ , where d is one-half of the thickness of the dielectric slab for the configuration being used.

The value of d for the empty guide and the 2x1/16 guide was simply taken to be half of the thickness of the center dielectric as defined. For the laminated guide and for the guide with round inserts, approximations were used. For the laminated guide the extra dielectric strips were disregarded in the calculation of d because of the similarity of the laminated guide with the empty guide (see Figure 4.1 or 4.2). The area of the cross section of the guide with the half round inserts was used to find an equivalent d (see Figure 3.2) that would produce an equal rectangular area with the width equal to the guide width. Values used for d are given in Table 4.1.



Table 4.1 Values of  $d$  for insert configurations.

Configuration	$d$
Empty guide	0.793 mm
2x1/16 inserts	2.381 mm
Round inserts	3.682 mm
Laminated guide	0.793 mm

The tabulated values of  $\alpha_z$  for many of the modes are given in Table 4.4.

Table 4.2 Mode numbers and their frequencies for the configurations.

mode	Wide empty	wide 2x1/16	wide round	wide laminated	narrow empty	narrow 2x1/16	narrow round	narrow lamin.
10					12.46			12.59
11				13.01	13.01			13.12
12	13.39			13.6	13.62	12.77		13.7
13	14.0	13.05		14.2	14.2	13.3		14.29
14	14.6	13.58	13.05	14.8	14.8	13.82		14.87
15	15.25	14.13	13.5	15.43	15.43	14.35	13.33	15.5
16	15.9	14.65	13.93	16.07	16.1	14.87	13.76	16.13
17	16.56	15.17	14.3	16.73	16.77	15.42	14.15	16.77
18	17.25	15.72	14.5	17.41	17.47	15.95	14.36	17.43
19		16.25	14.87			16.52	14.73	
20		16.8	15.33			17.07	15.18	
21		17.36	15.8			17.67	15.68	
22		17.93	16.28				16.13	
23			16.75				16.62	
24			17.23				17.12	
25			17.73				17.63	

Table 4.3 Q-Values

mode	wide empty	wide 2x1/16	wide round	wide lamin.	narrow empty	narrow 2x1/16	narrow round	narrow lamin.
10								
11								
12								
13	757	1900			1035			1427
14	1400			1480	792			1552
15	1040	900						
16		1465			807			1350
17	925	1625			940	1380		
18	800	1550		1310	995	1590		1609
19		1080	1215				735	
20								
21		786	765			1010		
22							1140	
23			1770					
24			886					
25							945	

**Page intentionally left blank**



[illegible]

### 4.3 Evaluation of $\alpha_x$

One of the characteristics of the H-guide structure is that the field intensities decrease exponentially with the distance from the dielectric slab. For walls of several wavelengths in height the energy radiated from the upper and lower openings is negligible. The results of measurements of the longitudinal field distribution as recorded on the XY plotter are illustrated in Figures 4.6 through 4.20. Representative field intensities and depths are labelled on the figures. From the curves of these figures the intensity was plotted for each depth. Plots are shown in Figures 4.4 and 4.5. The best linear curve was drawn through the data points (dash dot line). The slope of this line is the exponential field decay  $\alpha_x$  in the X direction. This procedure was repeated for each configuration, and the values are tabulated in Table 4.5. Since the field decrease near the slab is affected by loading, data points for the near-dielectric region were disregarded for the determination of the slope.



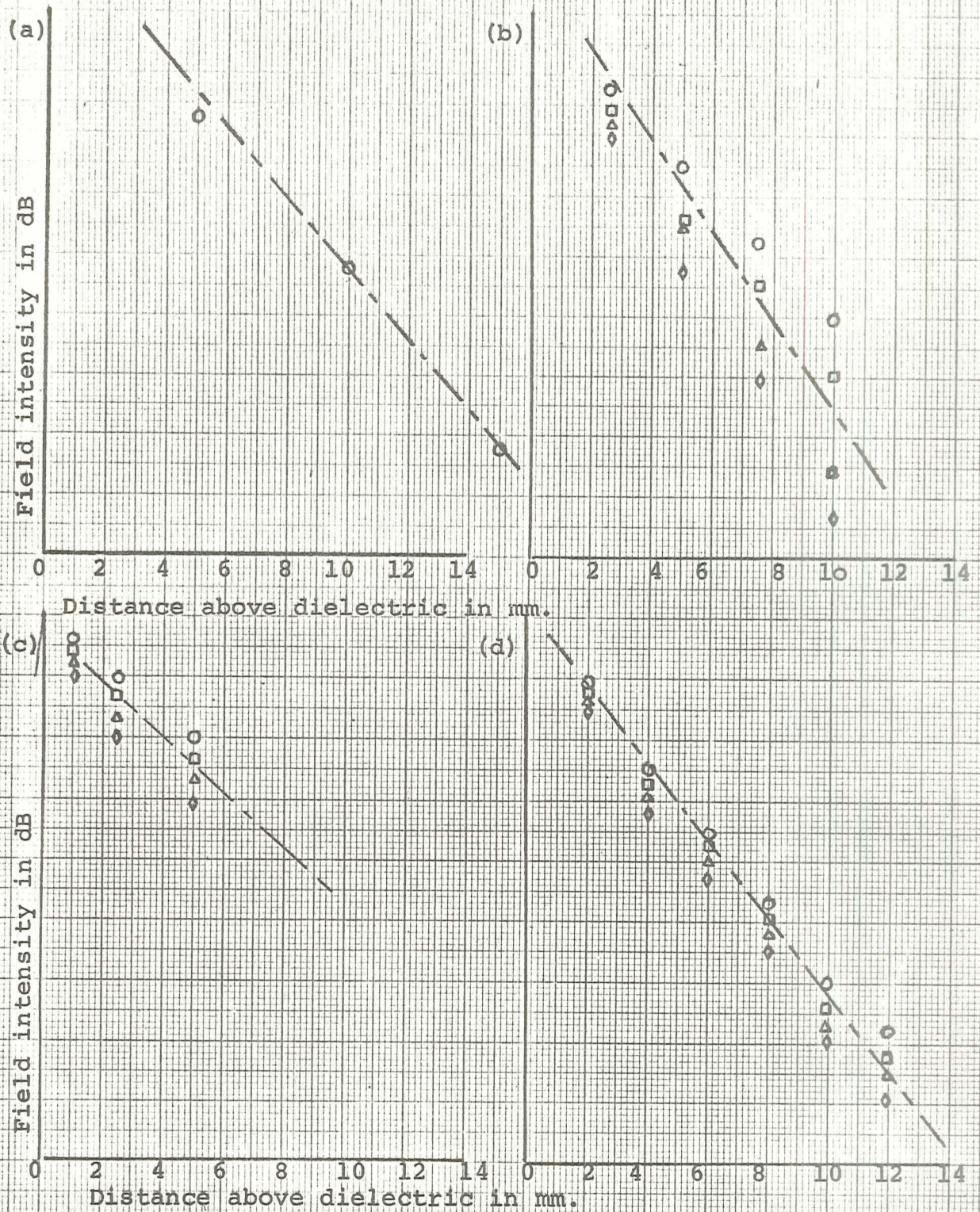


Figure 4.4 Vertical field decrease  $\alpha_z$  for; a) narrow empty, b) narrow 2x1/16, c) narrow round, and d) narrow laminated.



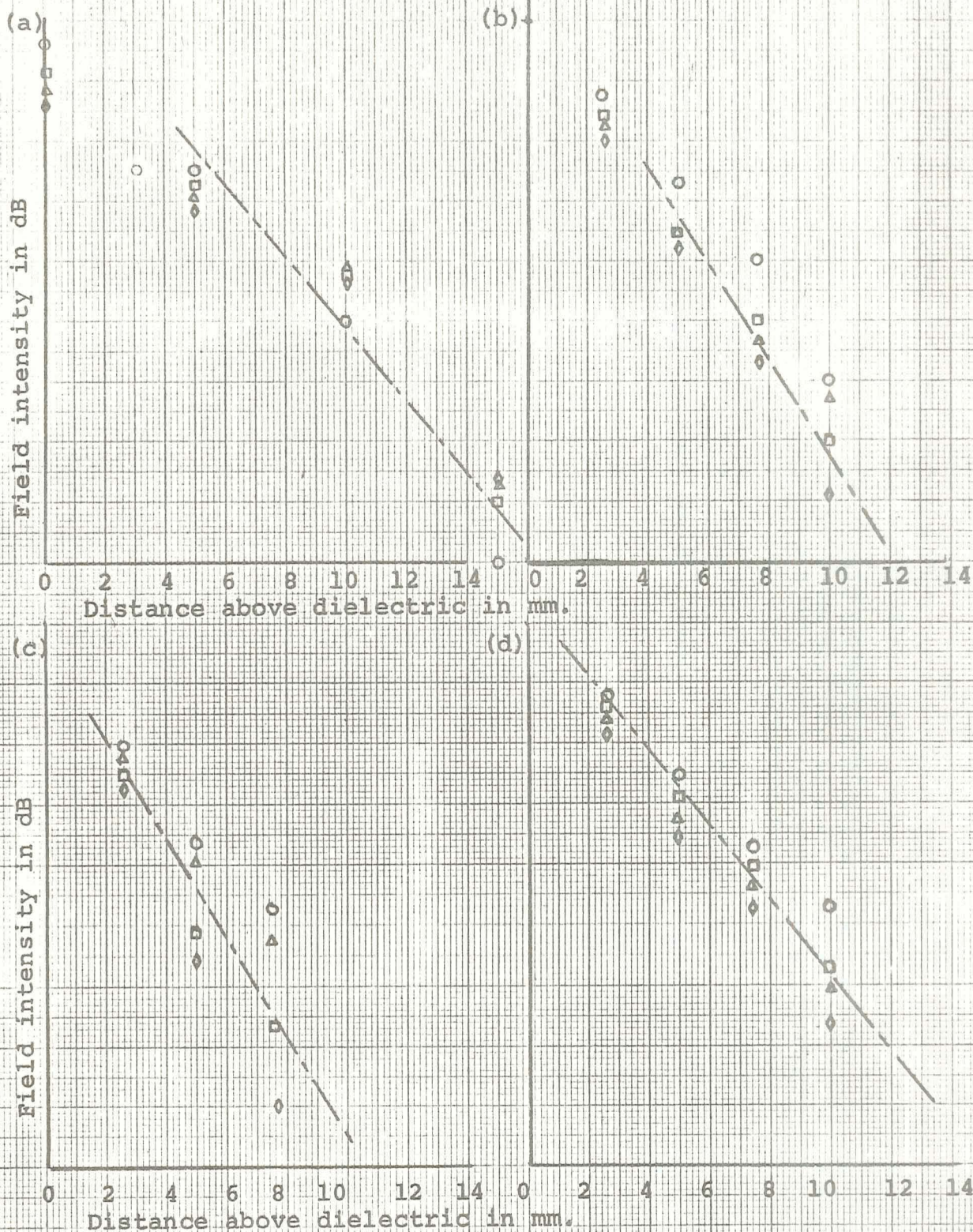
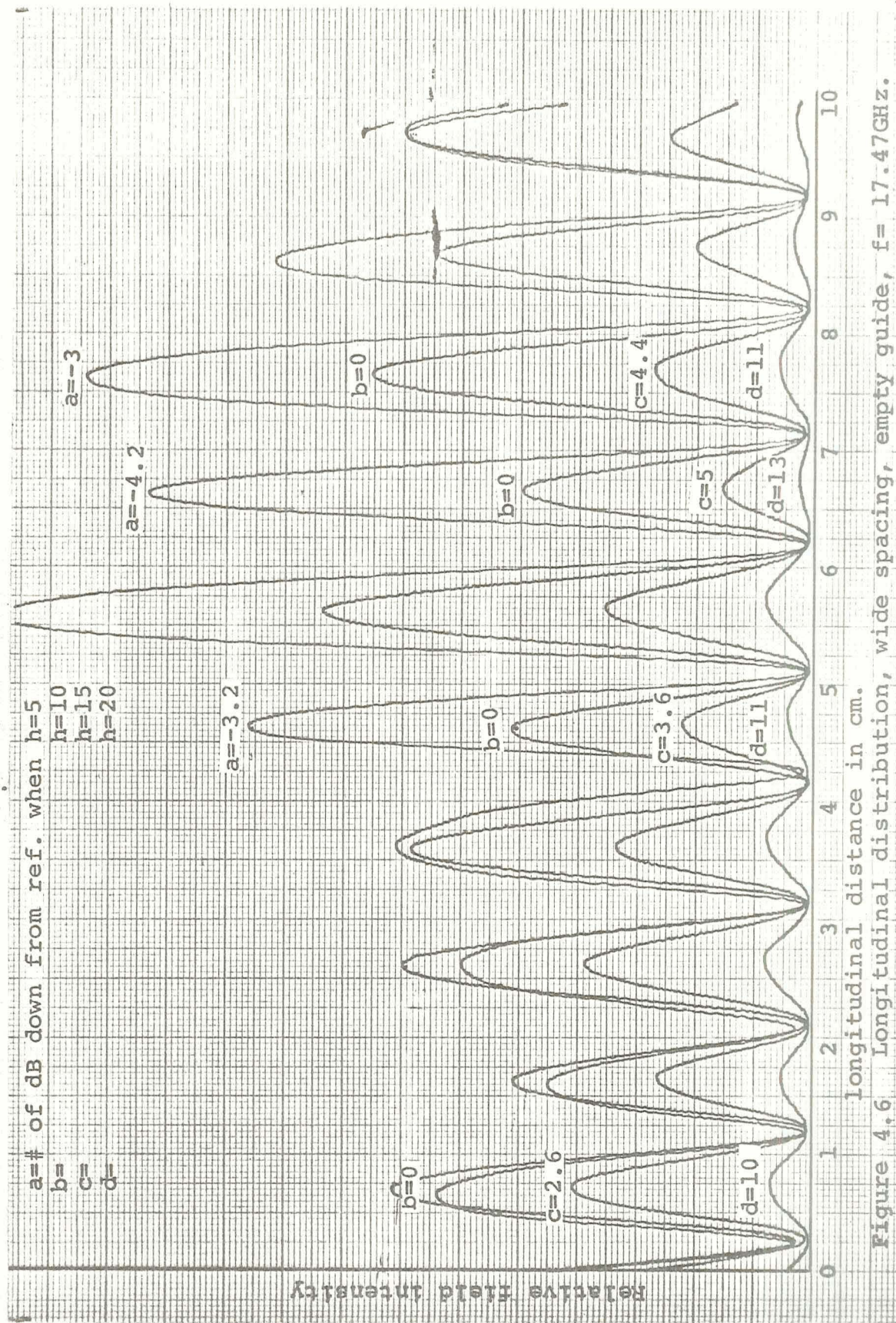


Figure 4.5 Vertical field decrease  $\alpha_z$  for; a) wide empty, b) wide 2x1/16, c) wide round, and d) wide laminated.



Table 4.5  $\alpha_x$  for various insert configurations

Configuration	$\alpha_x$ in dB/mm
wide empty	1.2
wide 2x1/16	1.62
wide round	1.62
wide laminated	1.225
narrow empty	1.18
narrow 2x1/16	1.516
narrow round	0.937
narrow laminated	1.27





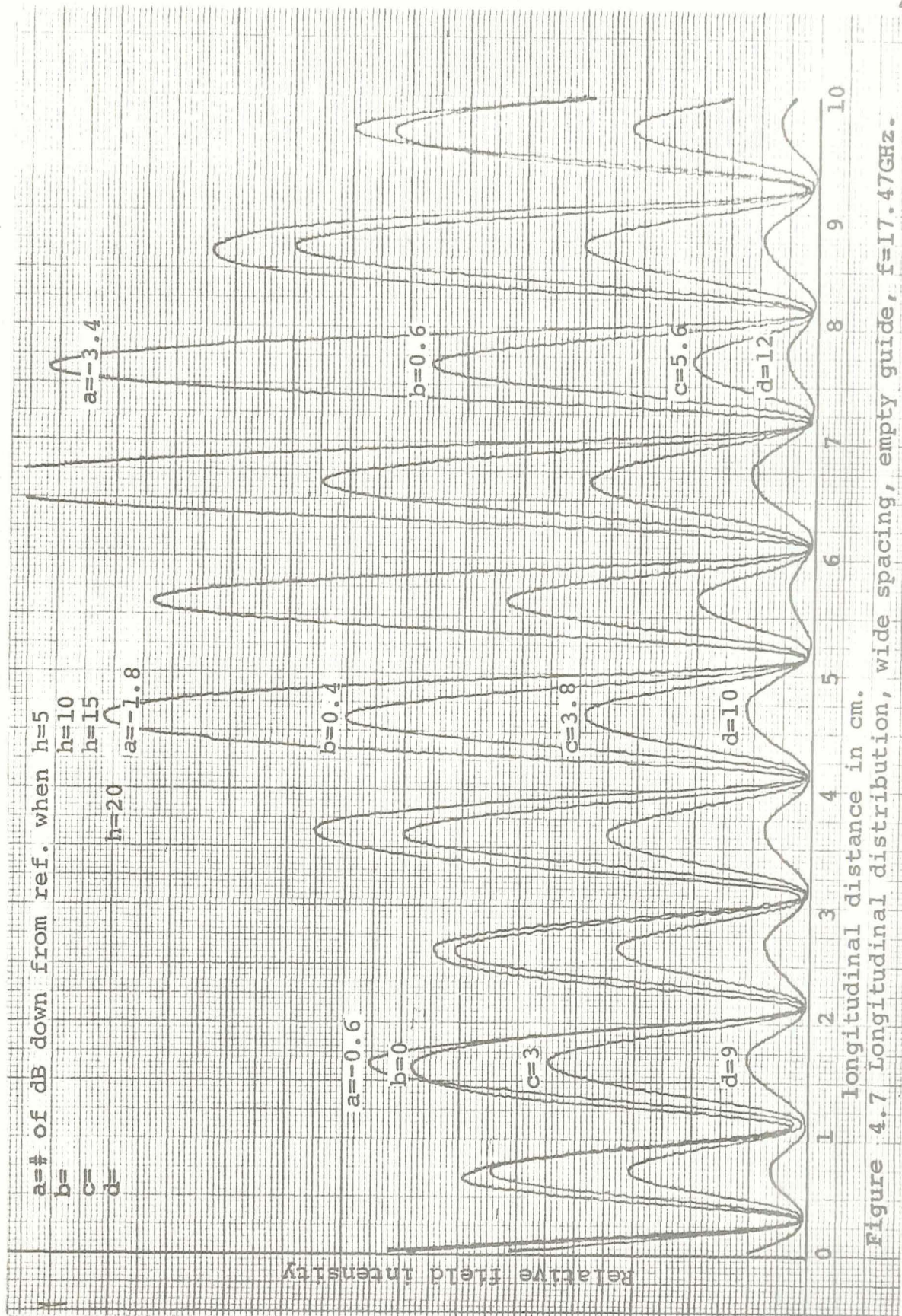
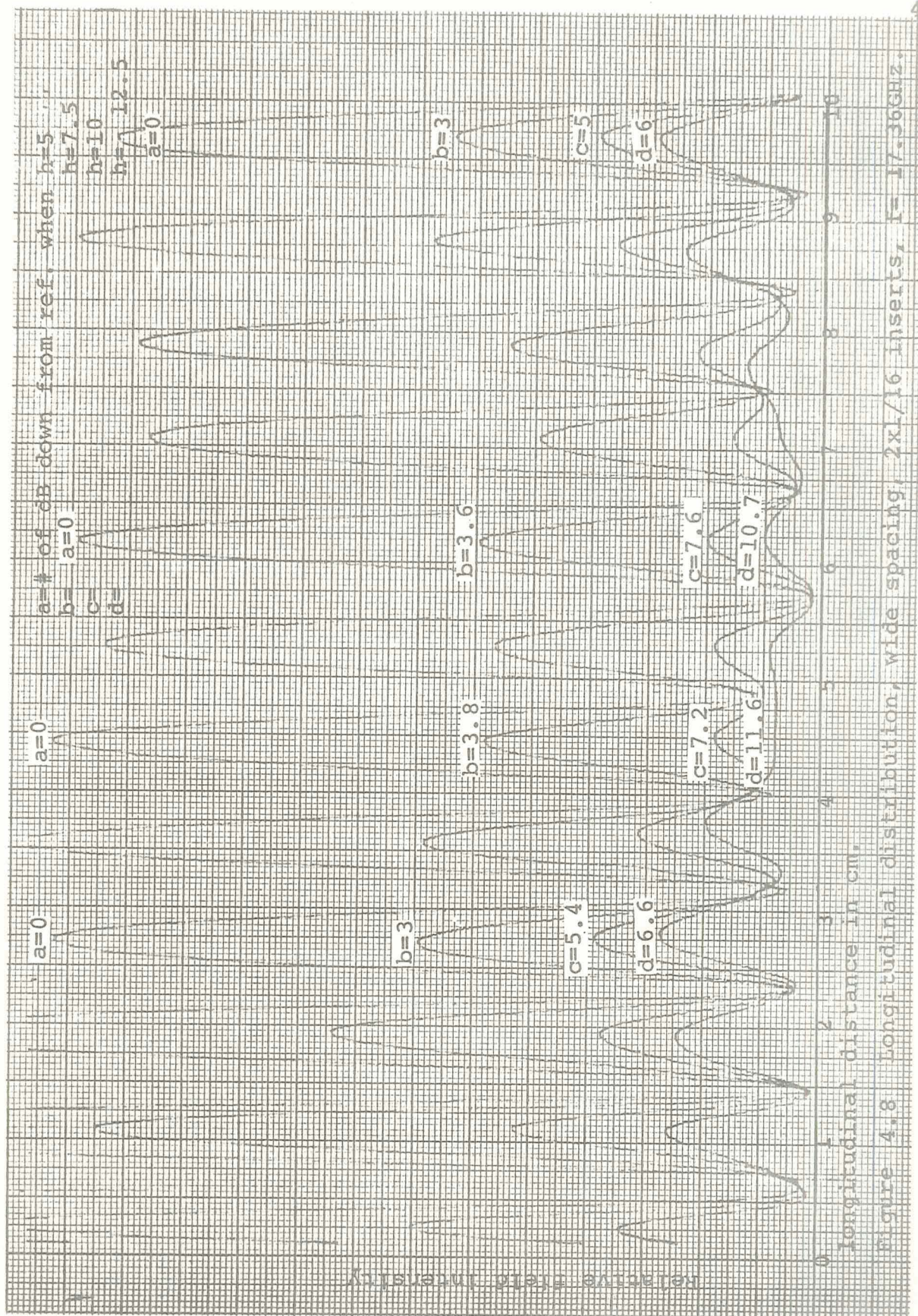


Figure 4.7 Longitudinal distribution, wide spacing, empty guide,  $f=17.47\text{GHz}$ .







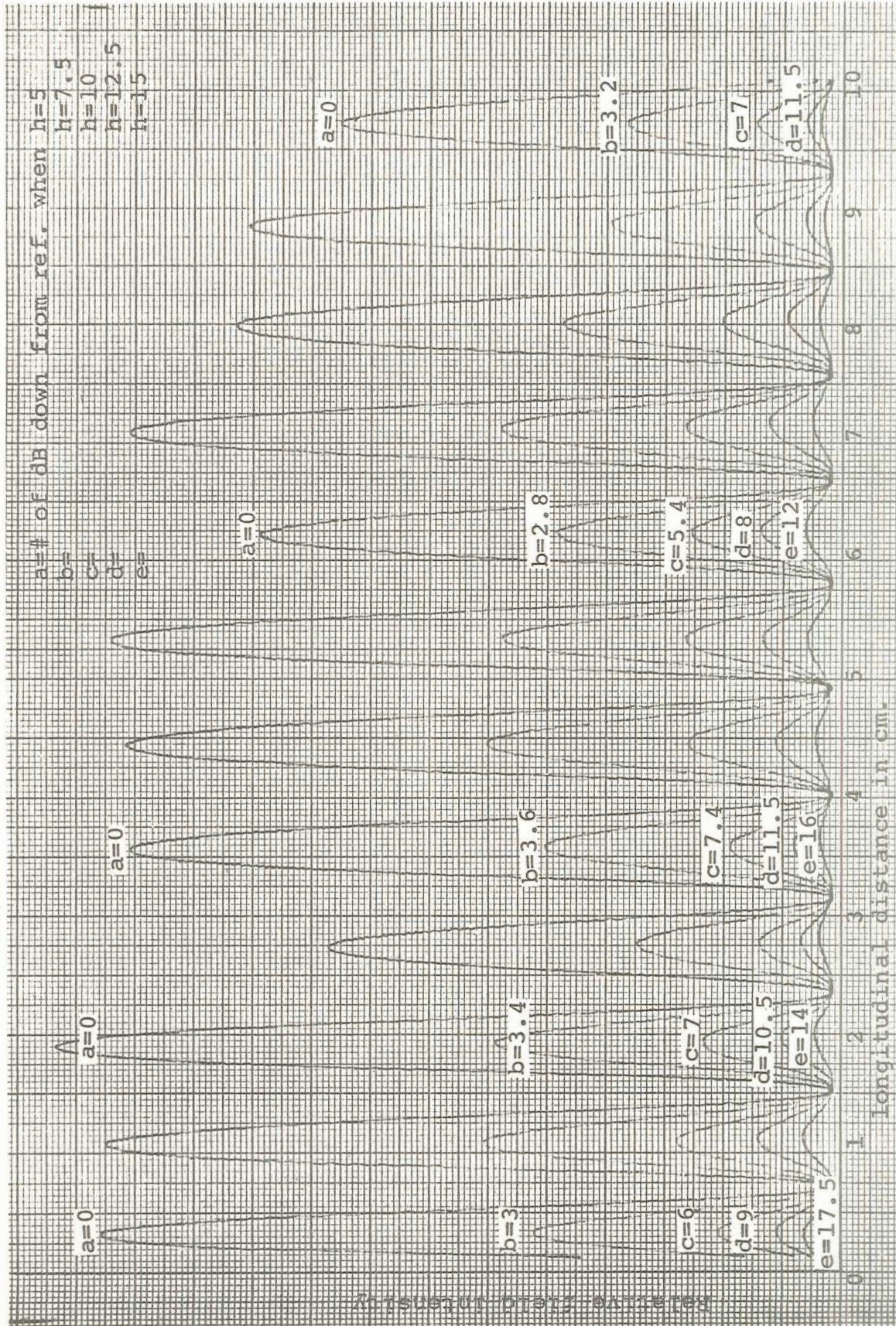
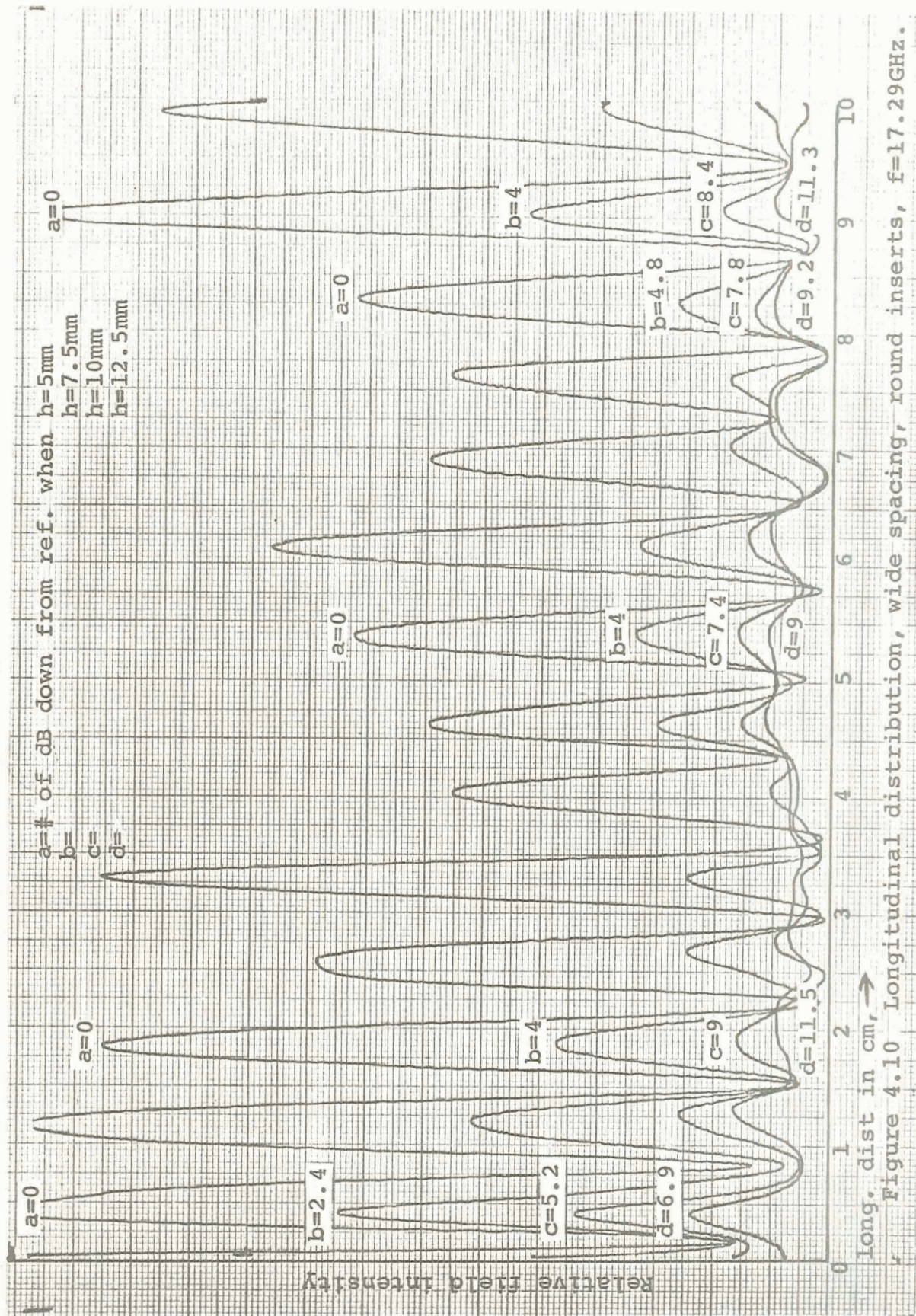


Figure 4.9 Longitudinal distribution, wide spacing, 2x1/16 inserts,  $f=17.36\text{GHz}$ .







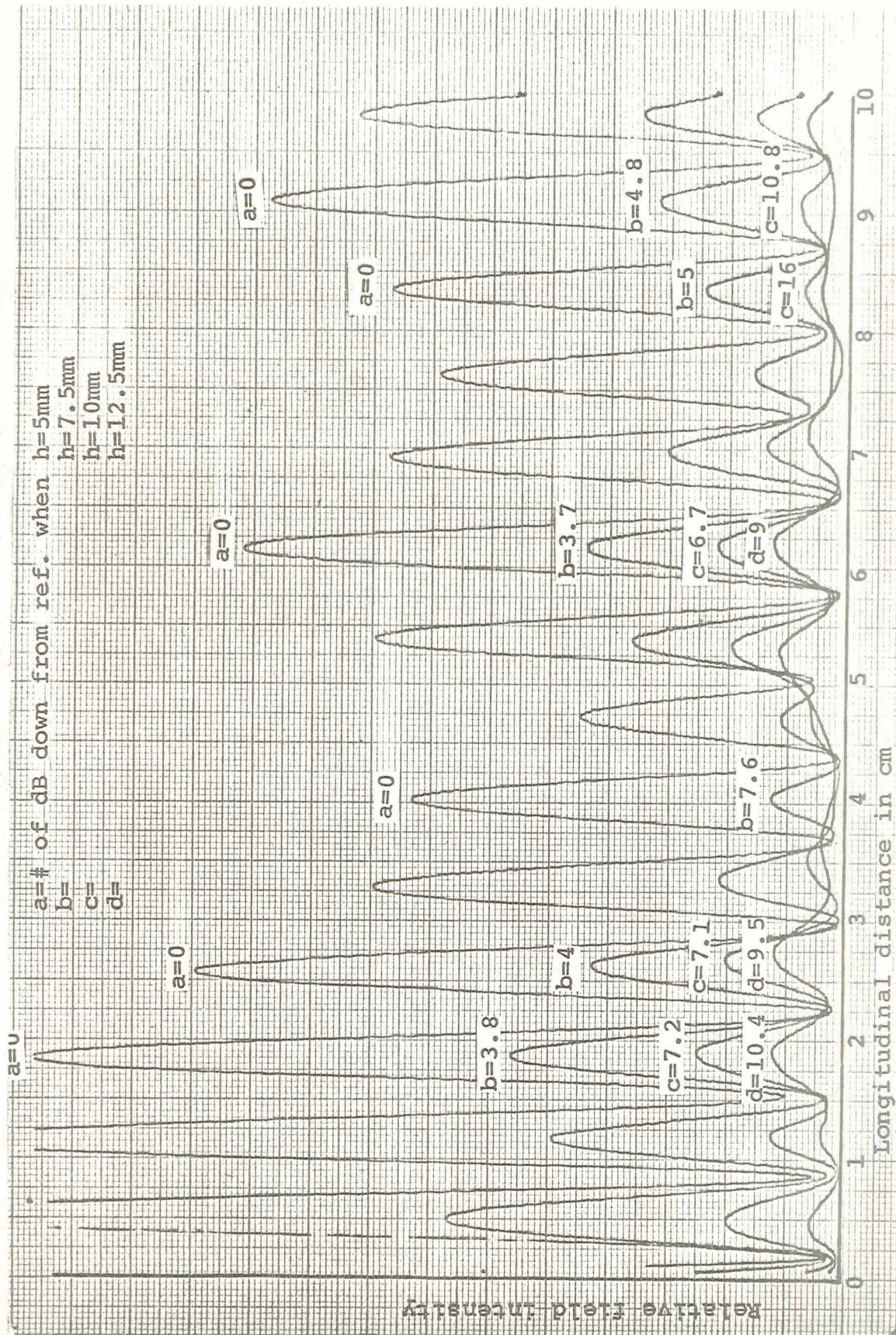


Figure 4.11 Longitudinal distribution, wide spacing, round inserts,  $f = 17.29\text{GHz}$ .



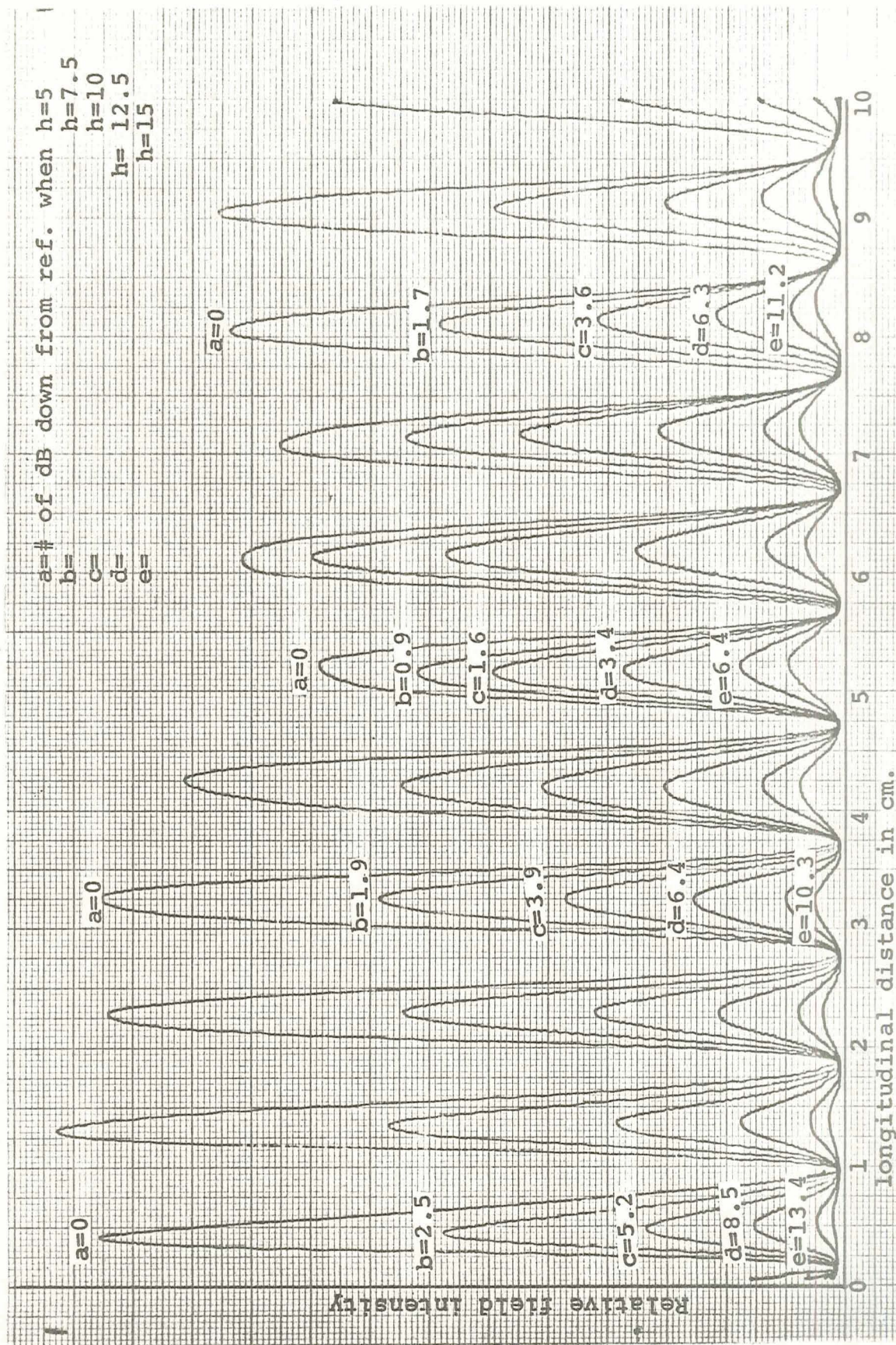


Figure 4.12 Longitudinal distribution, wide spacing, laminated guide,  $f=17.41\text{GHz}$ .



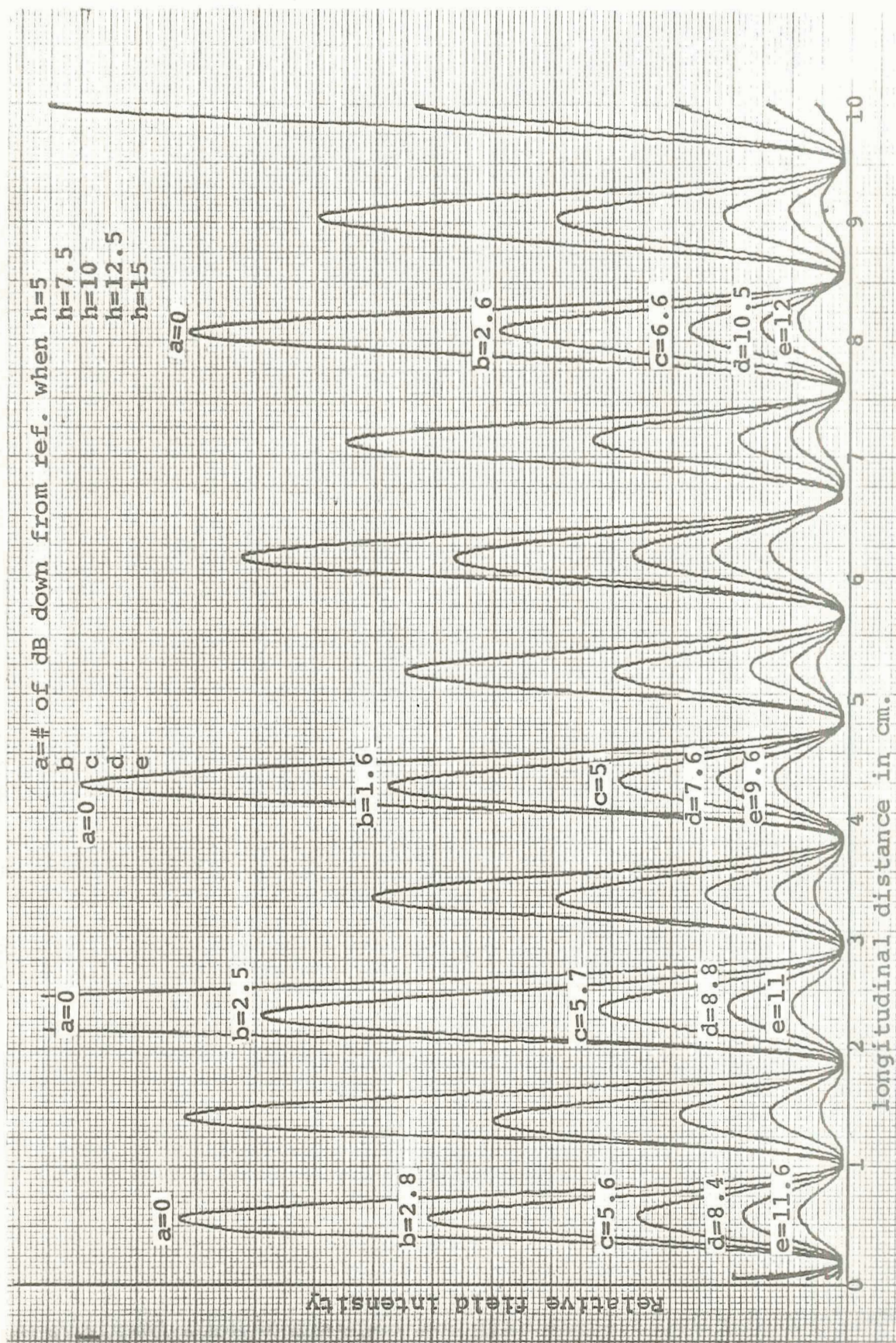


Figure 4.13 Longitudinal distribution, wide spacing, laminated guide,  $f=17.41\text{GHz}$ .



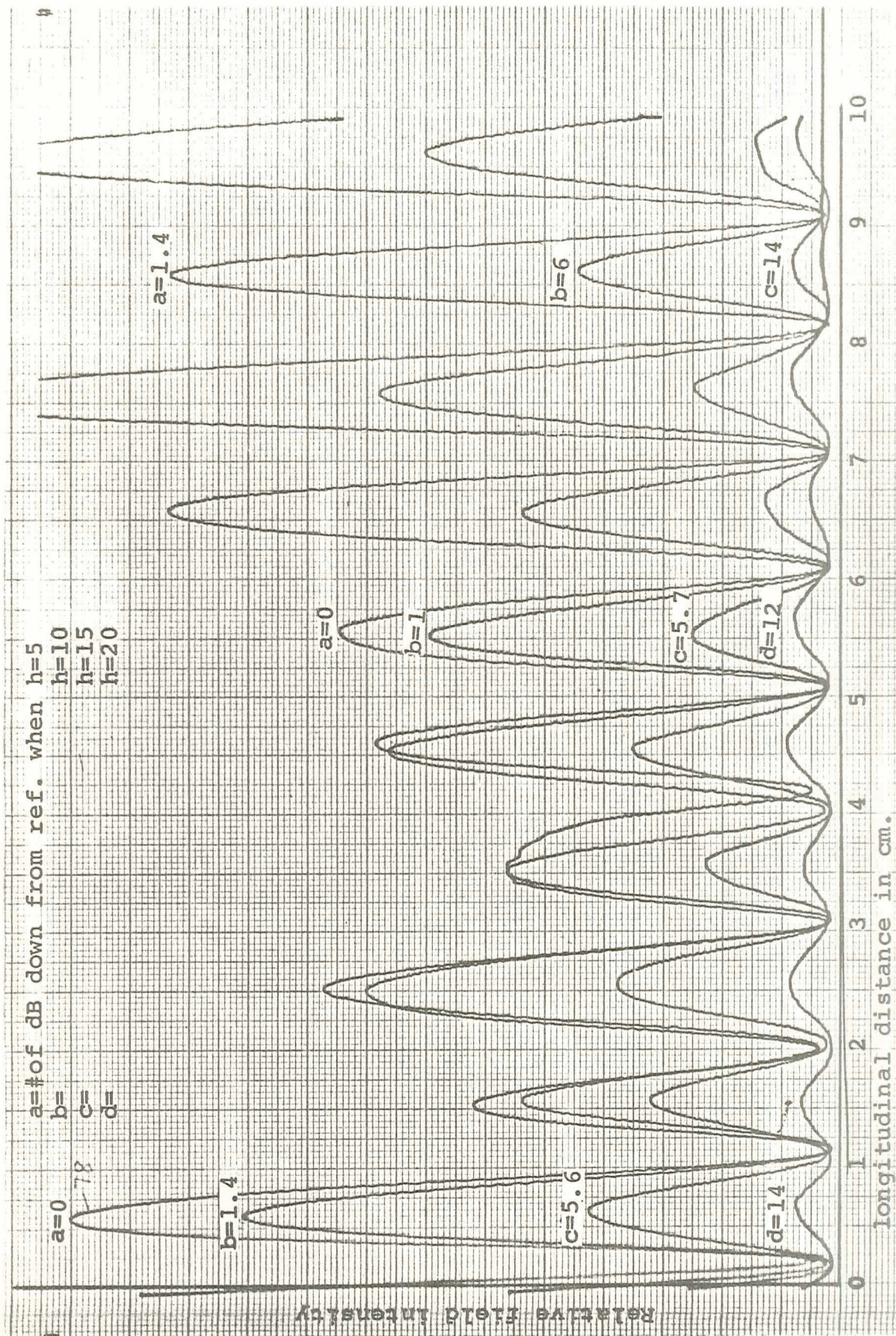
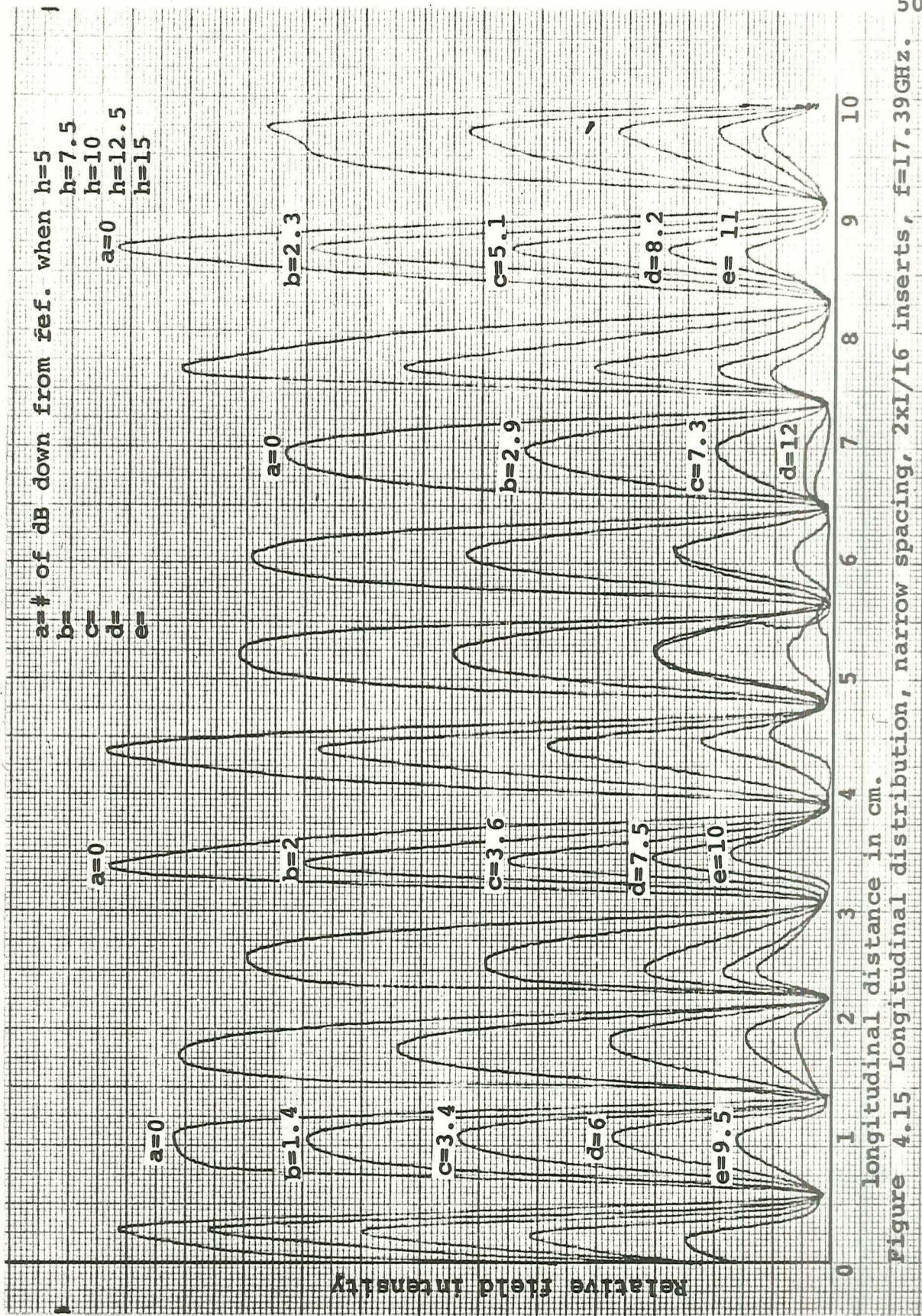


Figure 4.14 Longitudinal distribution, narrow spacing, empty guide,  $f=17.47\text{GHz}$ .







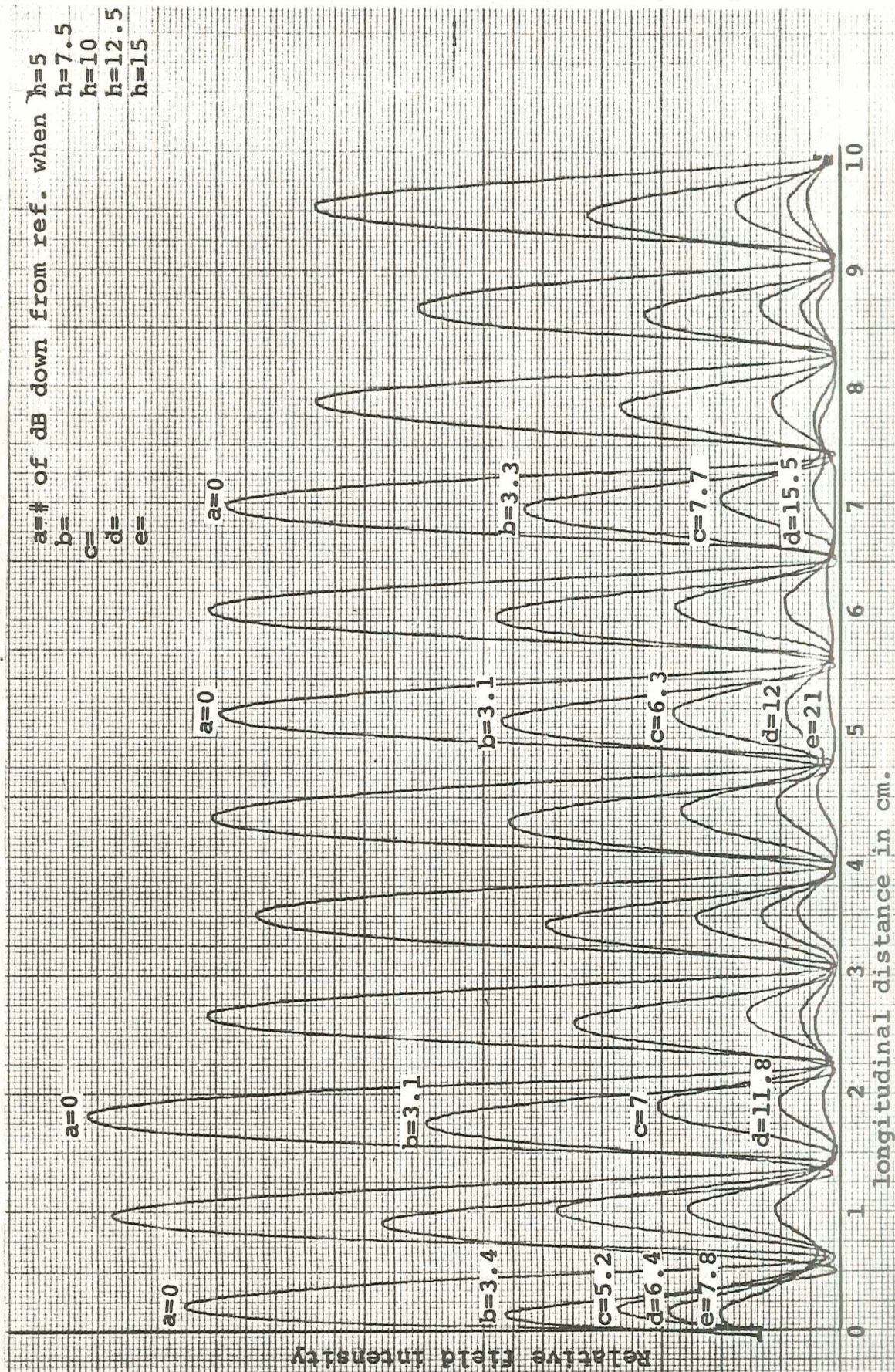


Figure 4.16 Longitudinal distribution, narrow spacing, 2x1/16 inserts,  $f=17.39\text{GHz}$ .



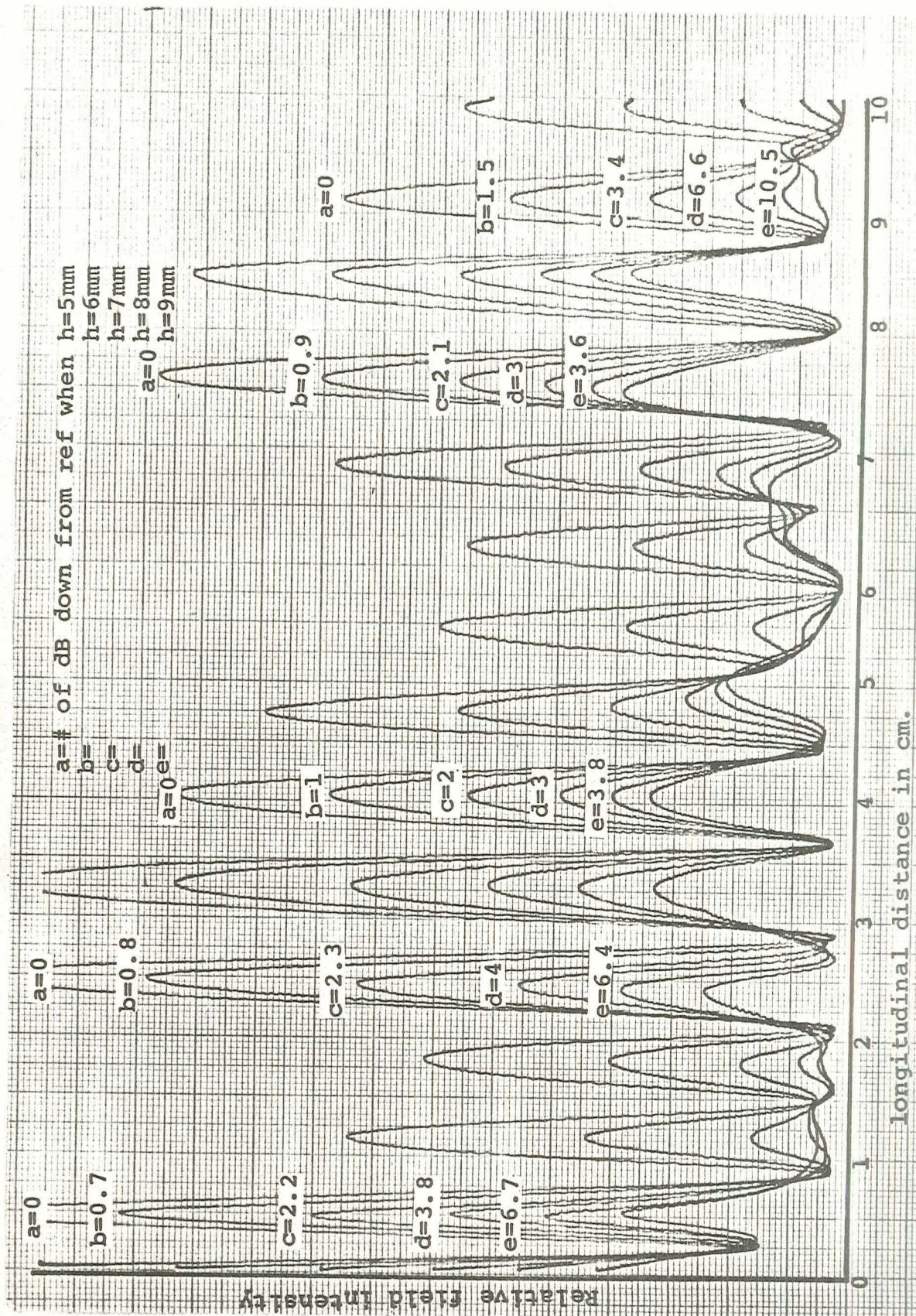


Figure 4.17 Longitudinal distribution, narrow spacing, round inserts,  $f=17.1$ .



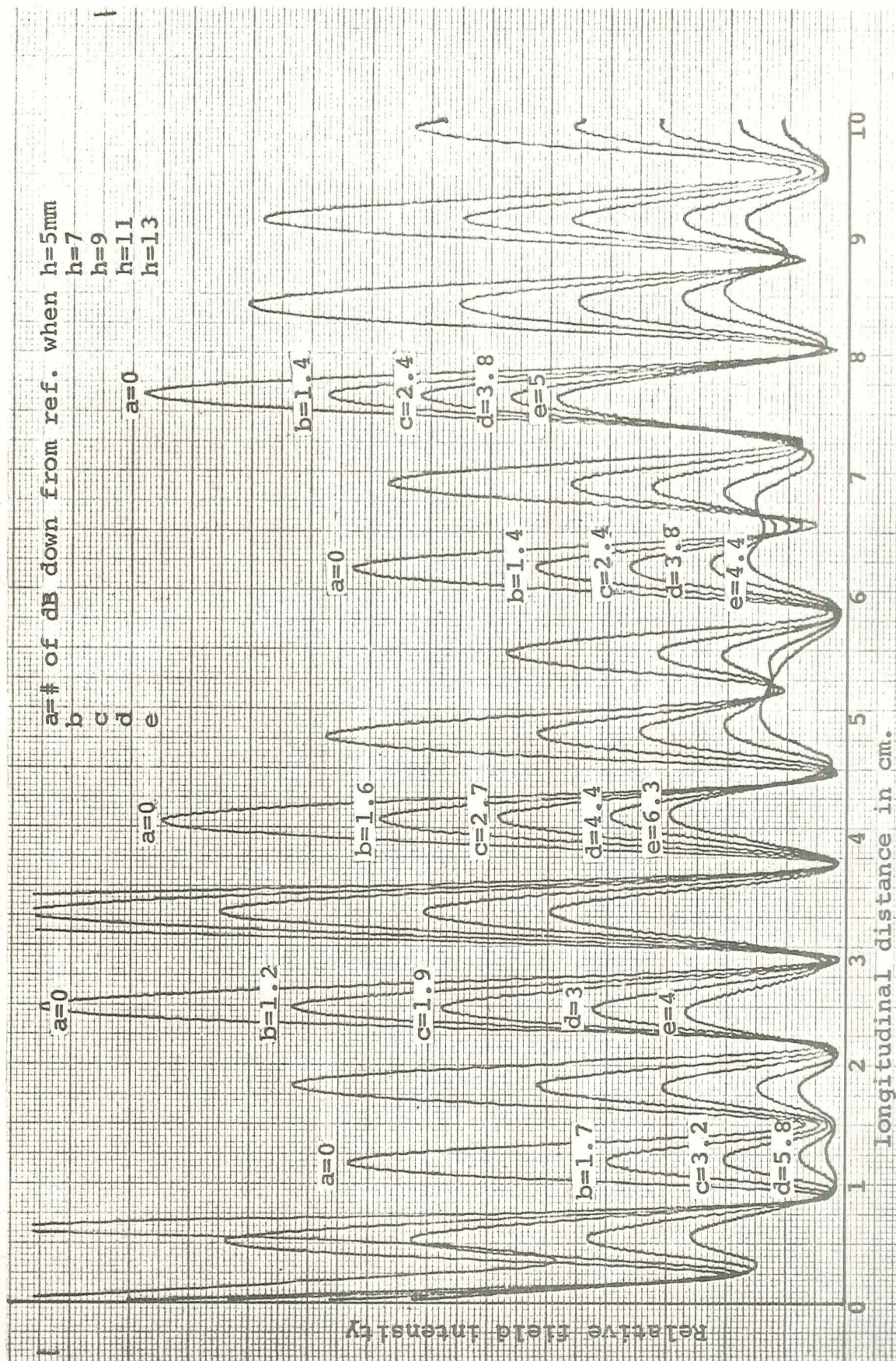


Figure 4.18 Longitudinal distribution, narrow spacing, round inserts,  $f=17.1\text{GHz}$ .



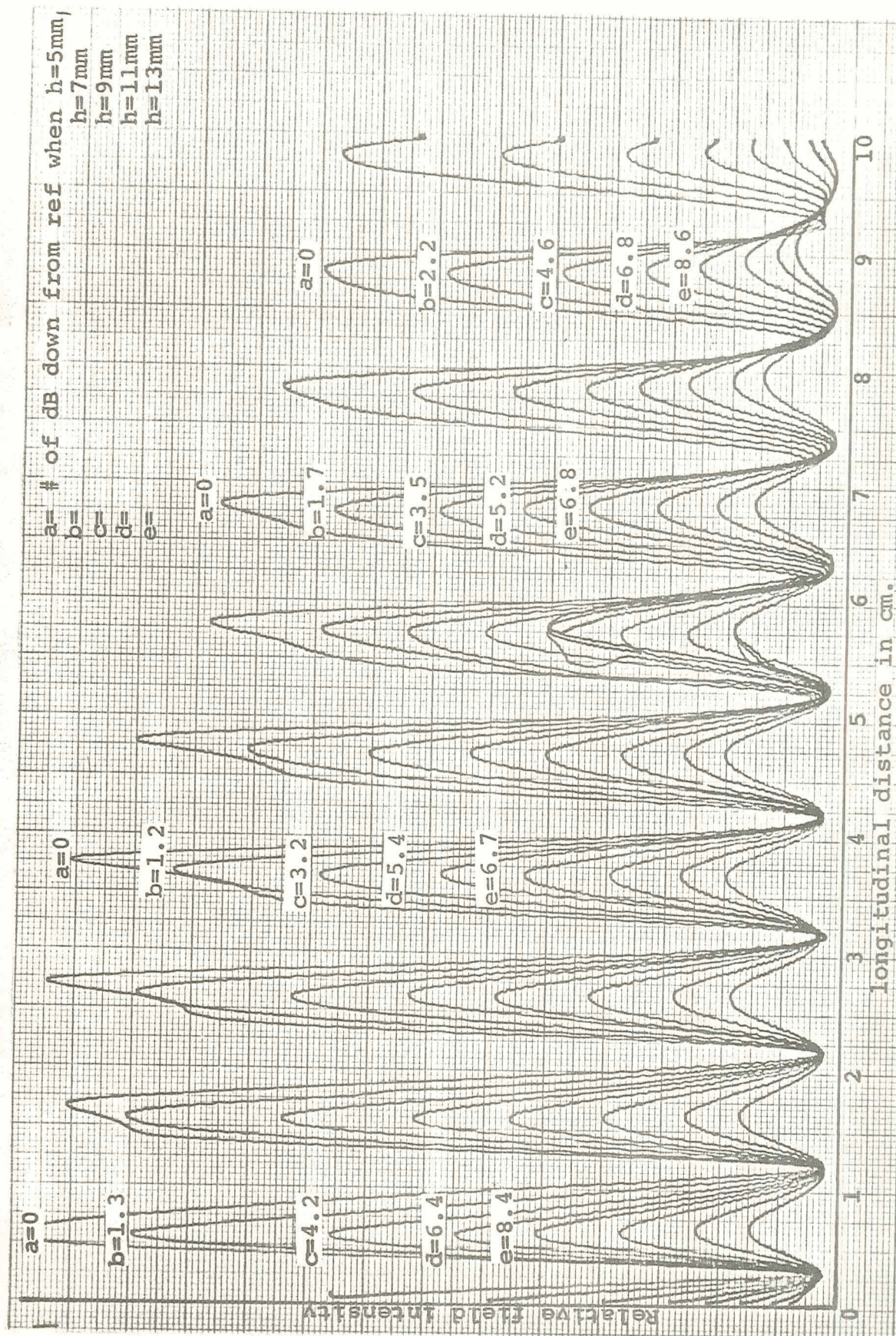


Figure 4.19 Longitudinal distribution, narrow spacing, laminated guide,  $f=17.0\text{GHz}$ .



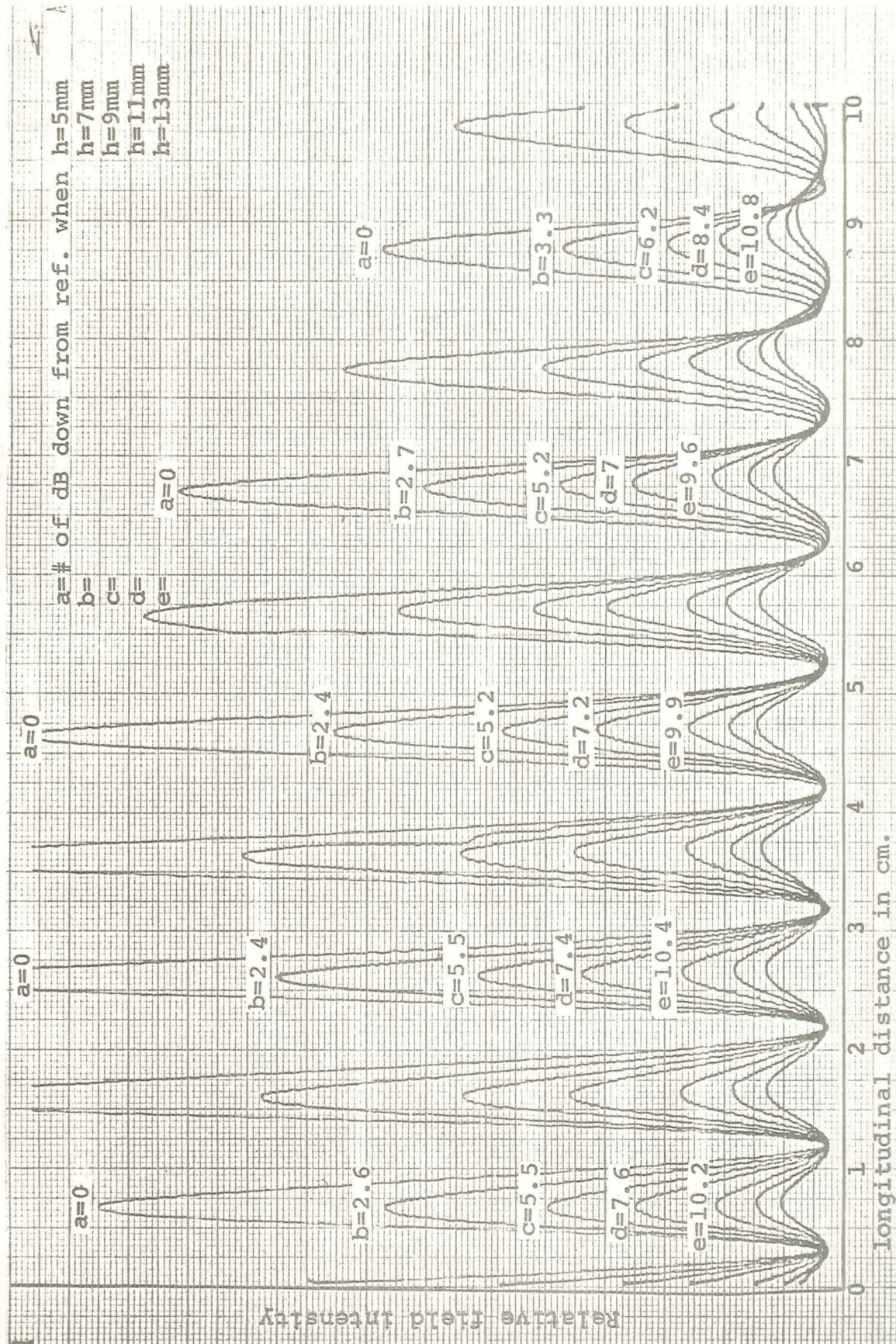


Figure 4.20 Longitudinal distribution, narrow spacing, laminated guide,  $f=17.0\text{GHz}$ .



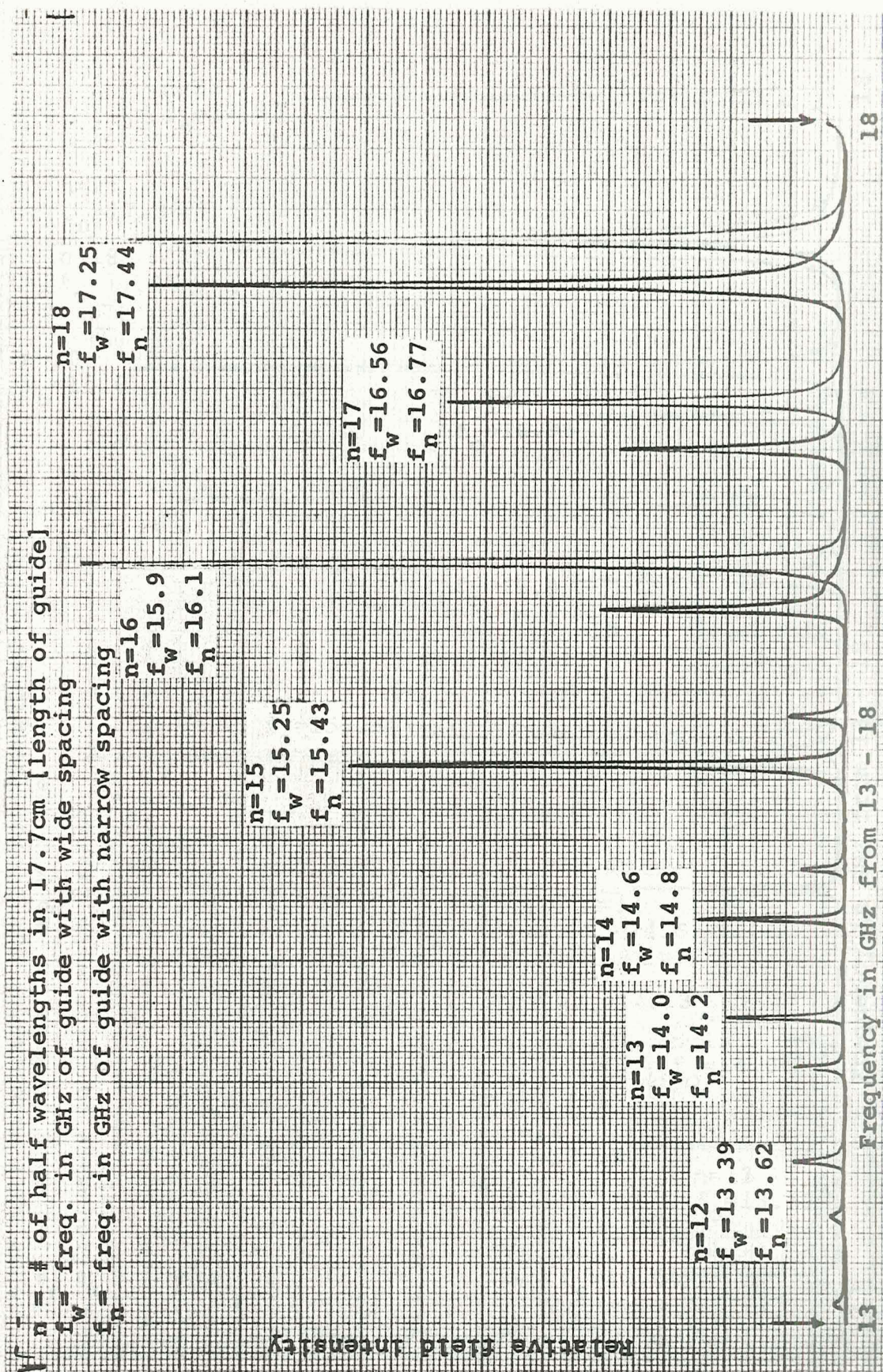
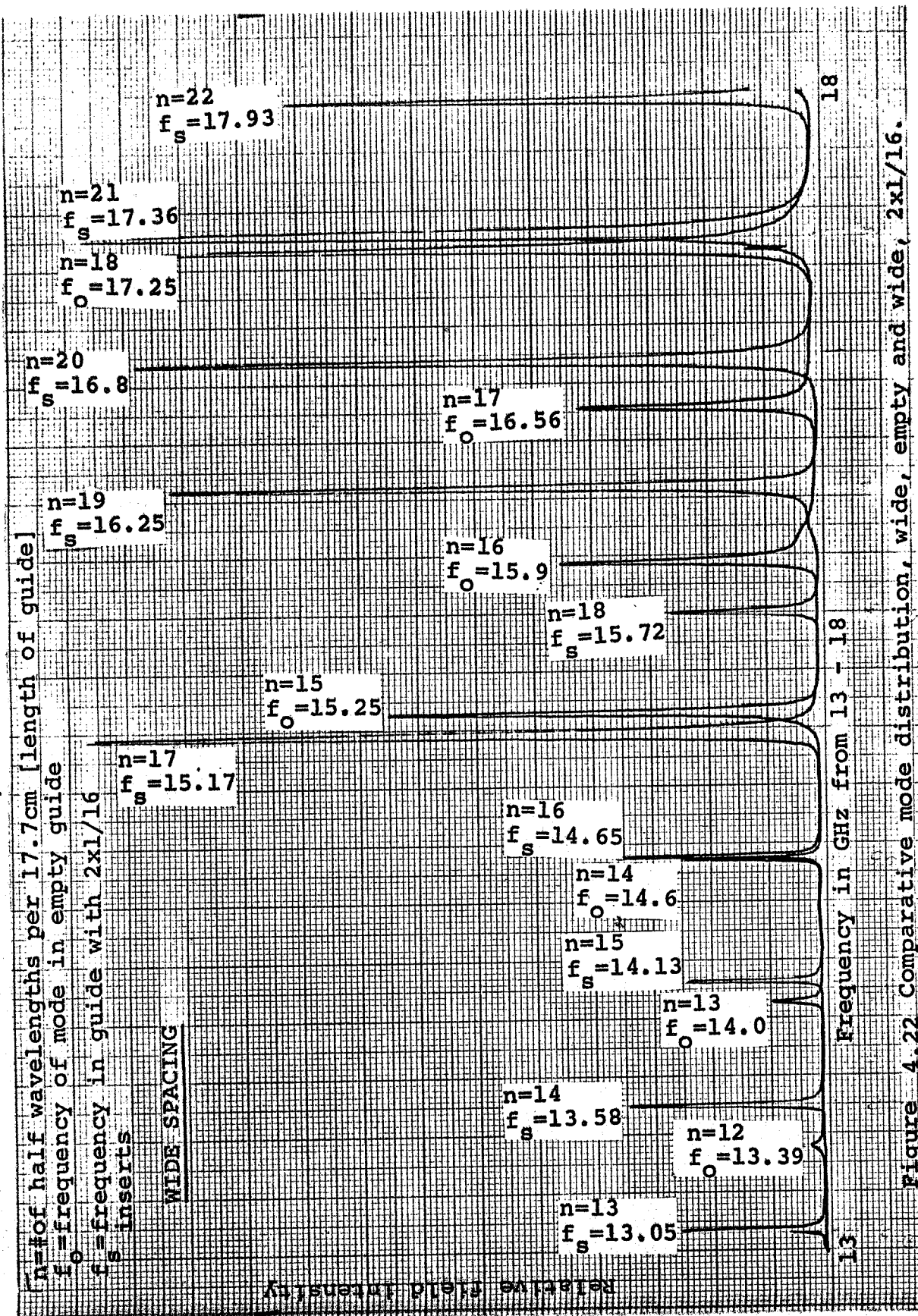


Figure 4.21 Comparative mode distribution, wide, empty and narrow, empty.







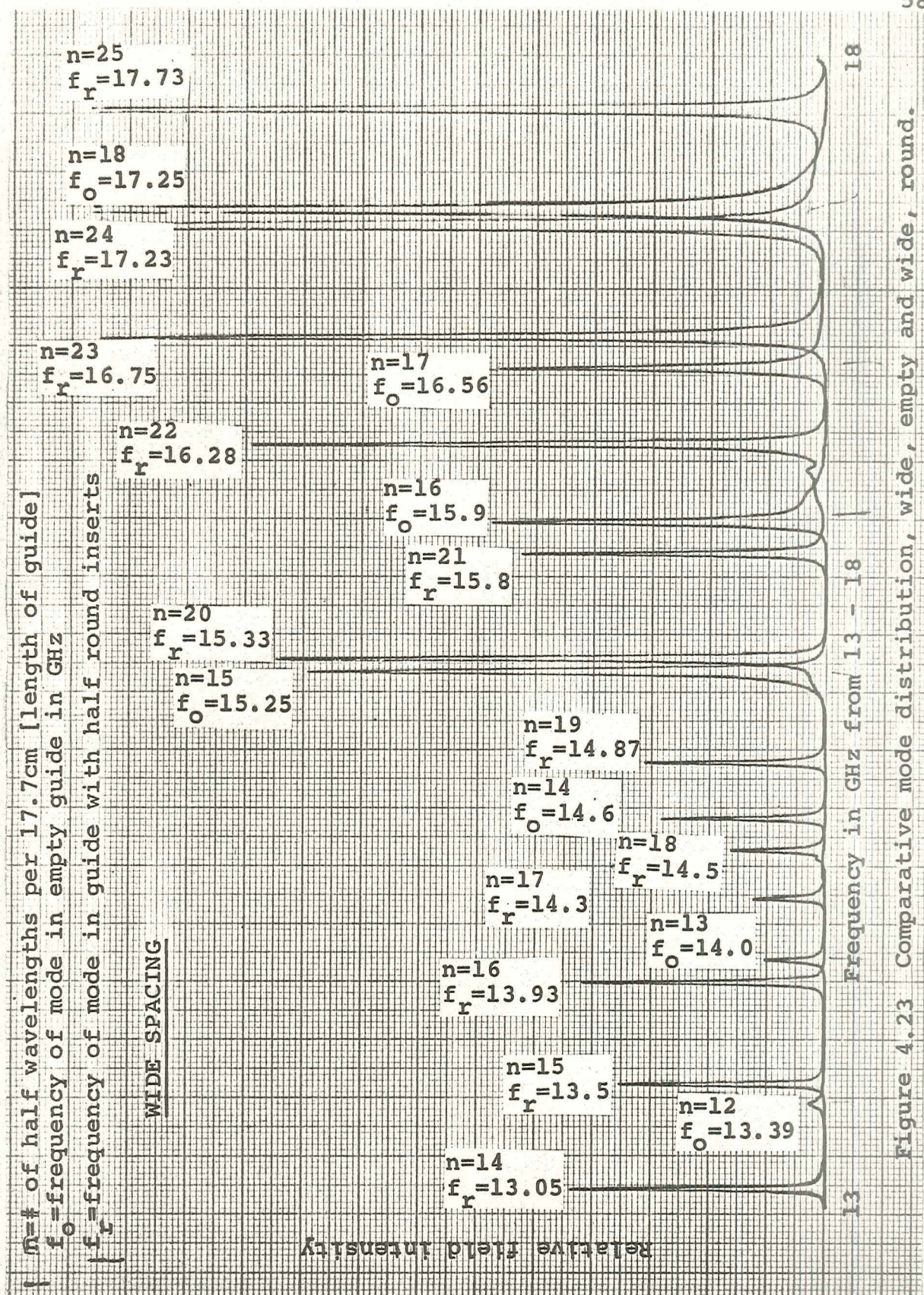


Figure 4.23 Comparative mode distribution, wide, empty and wide, round.



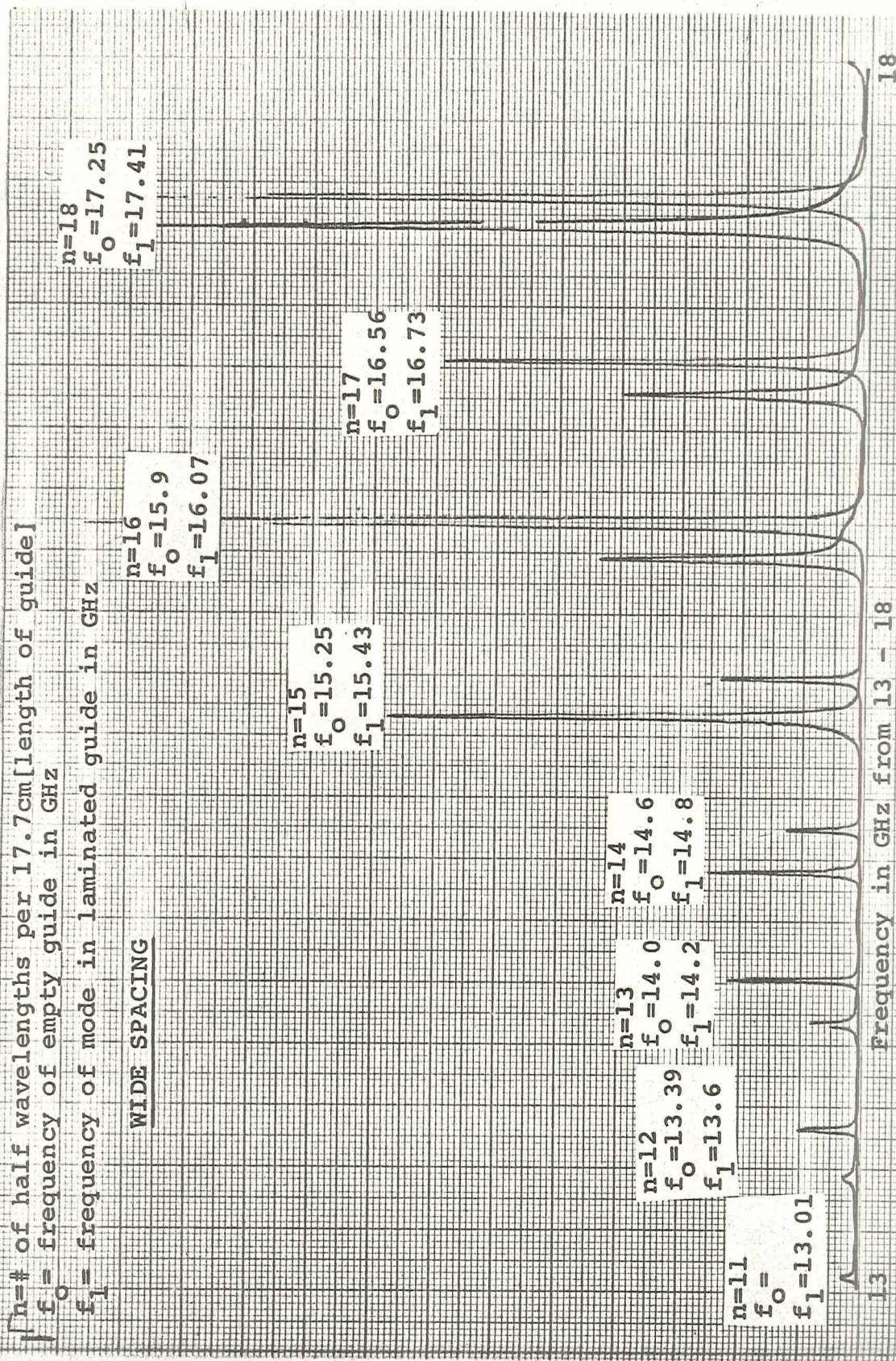


Figure 4.24 Comparative mode distribution, wide, empty and wide, laminated.



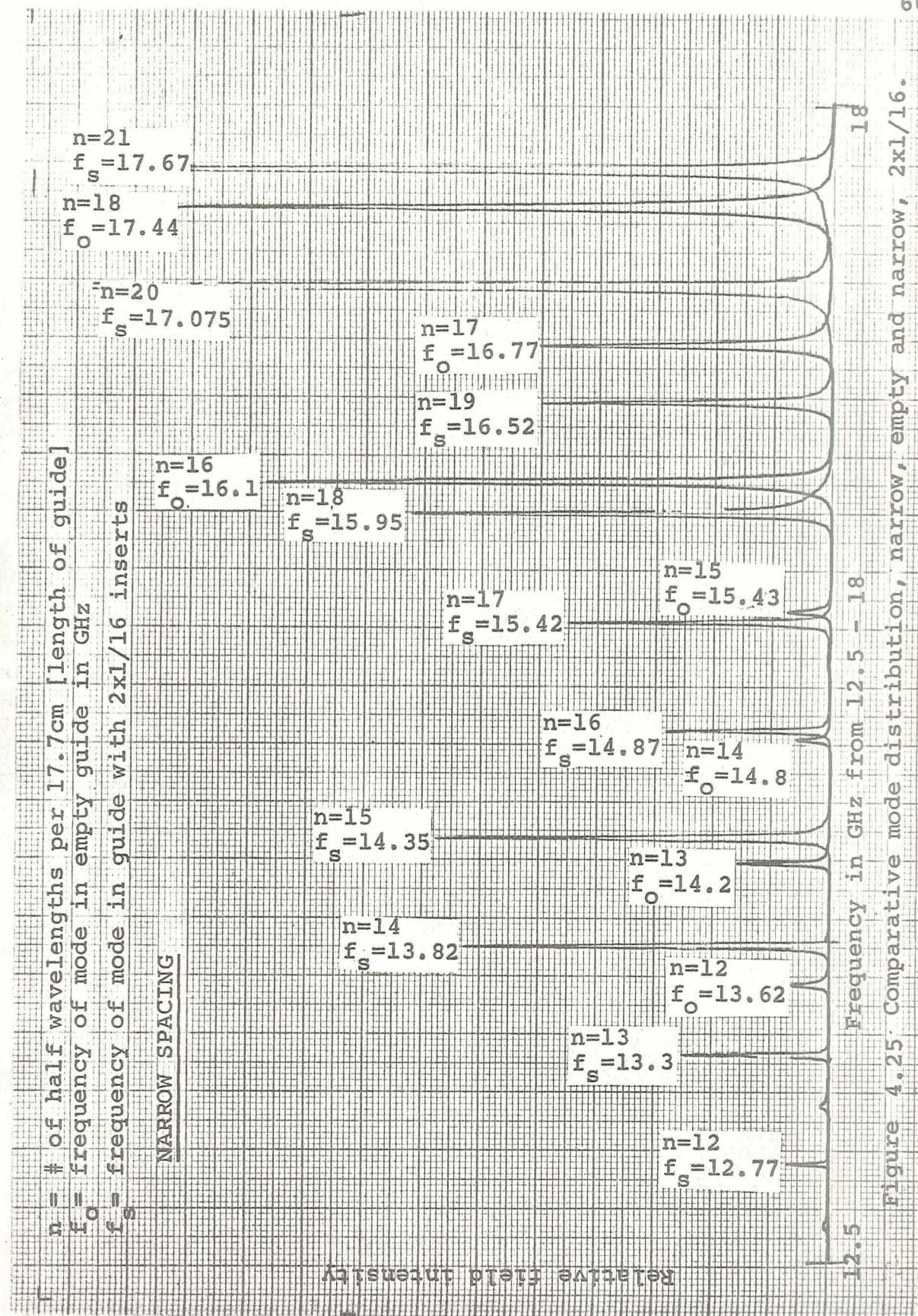


Figure 4.25 Comparative mode distribution, narrow, empty and narrow, 2x1/16.



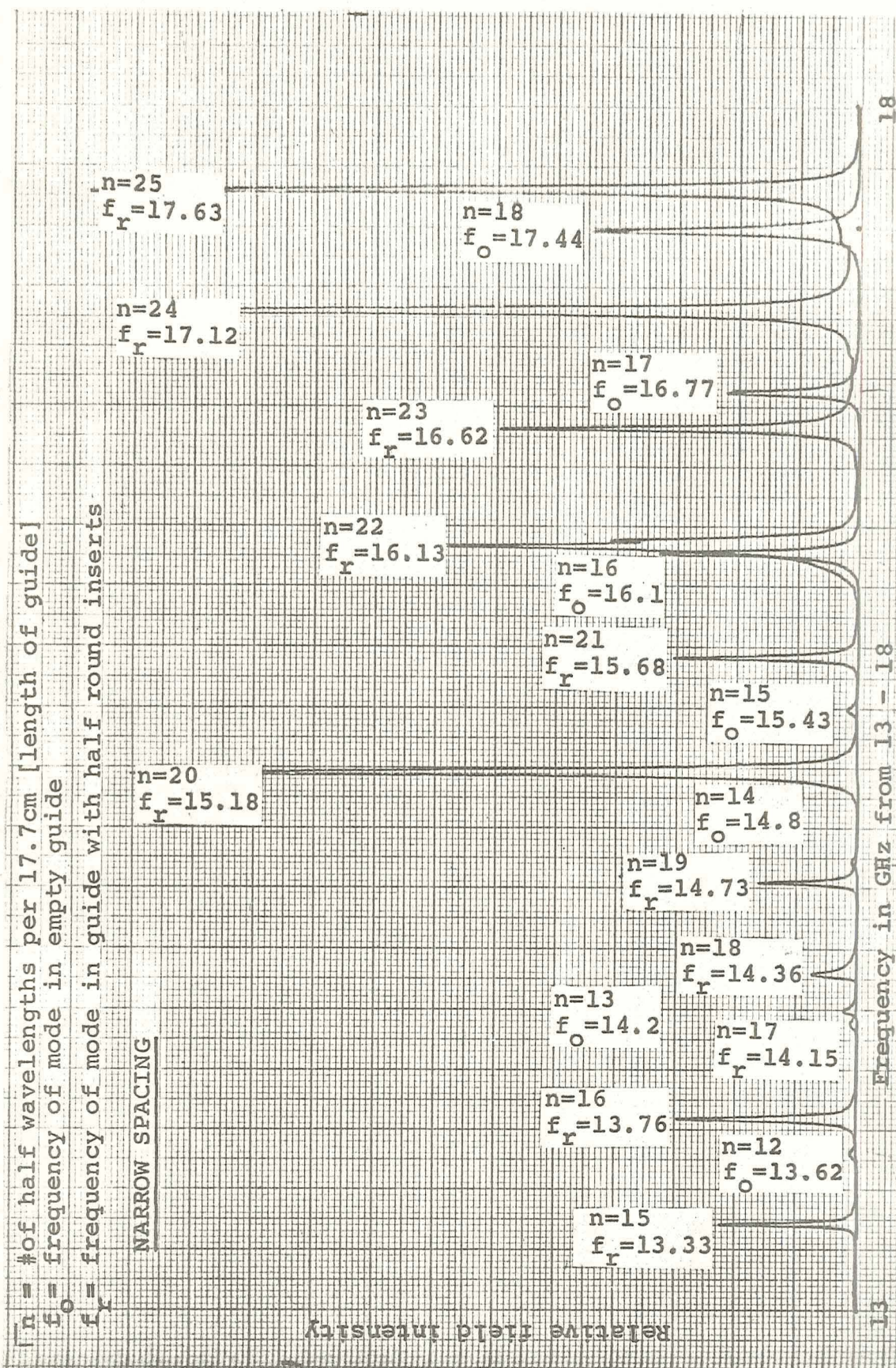


Figure 4.26 comparative mode distribution, narrow, empty and narrow, round.



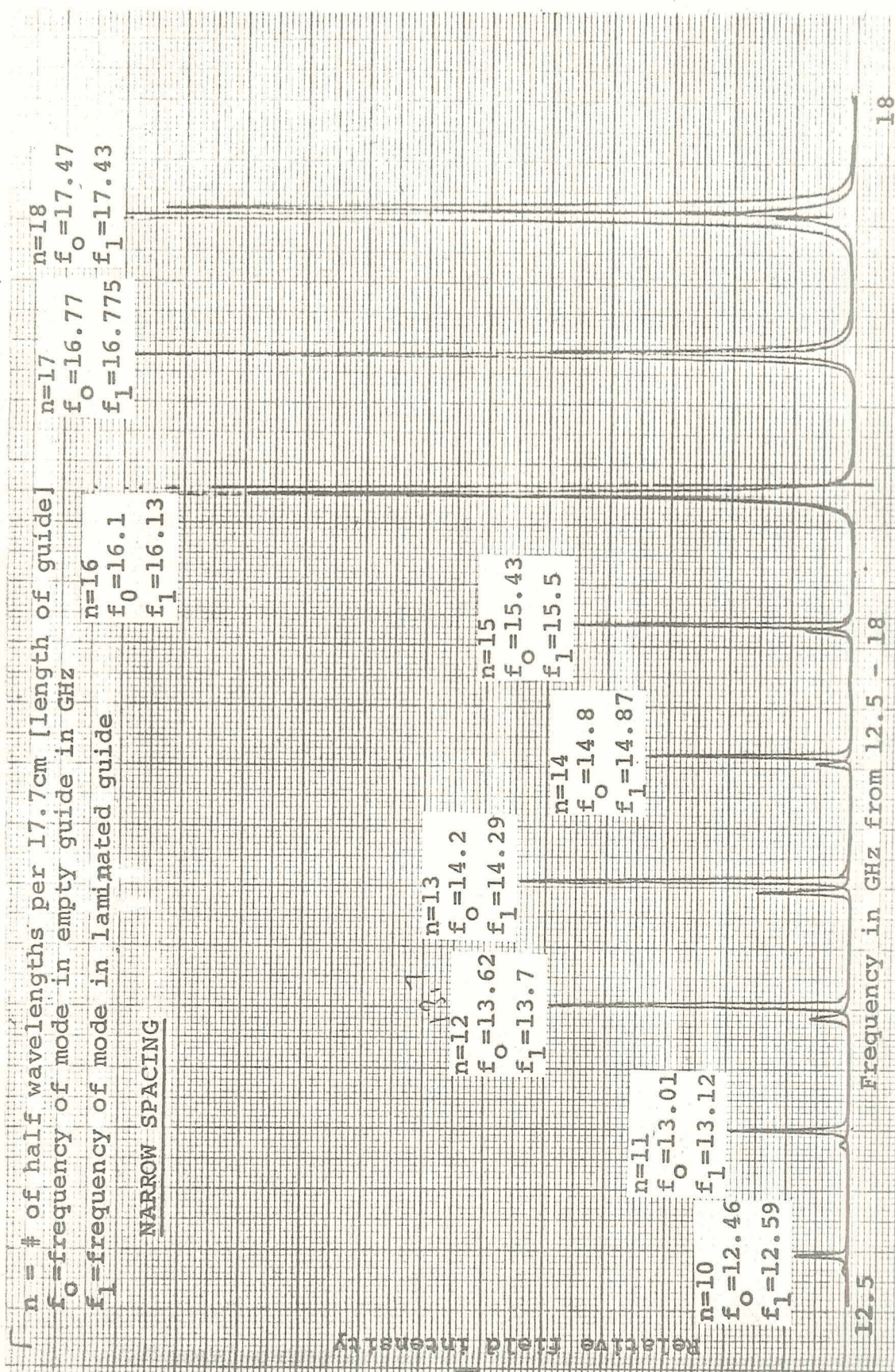


Figure 4.27 Comparative mode distribution, narrow, empty and narrow, laminated.



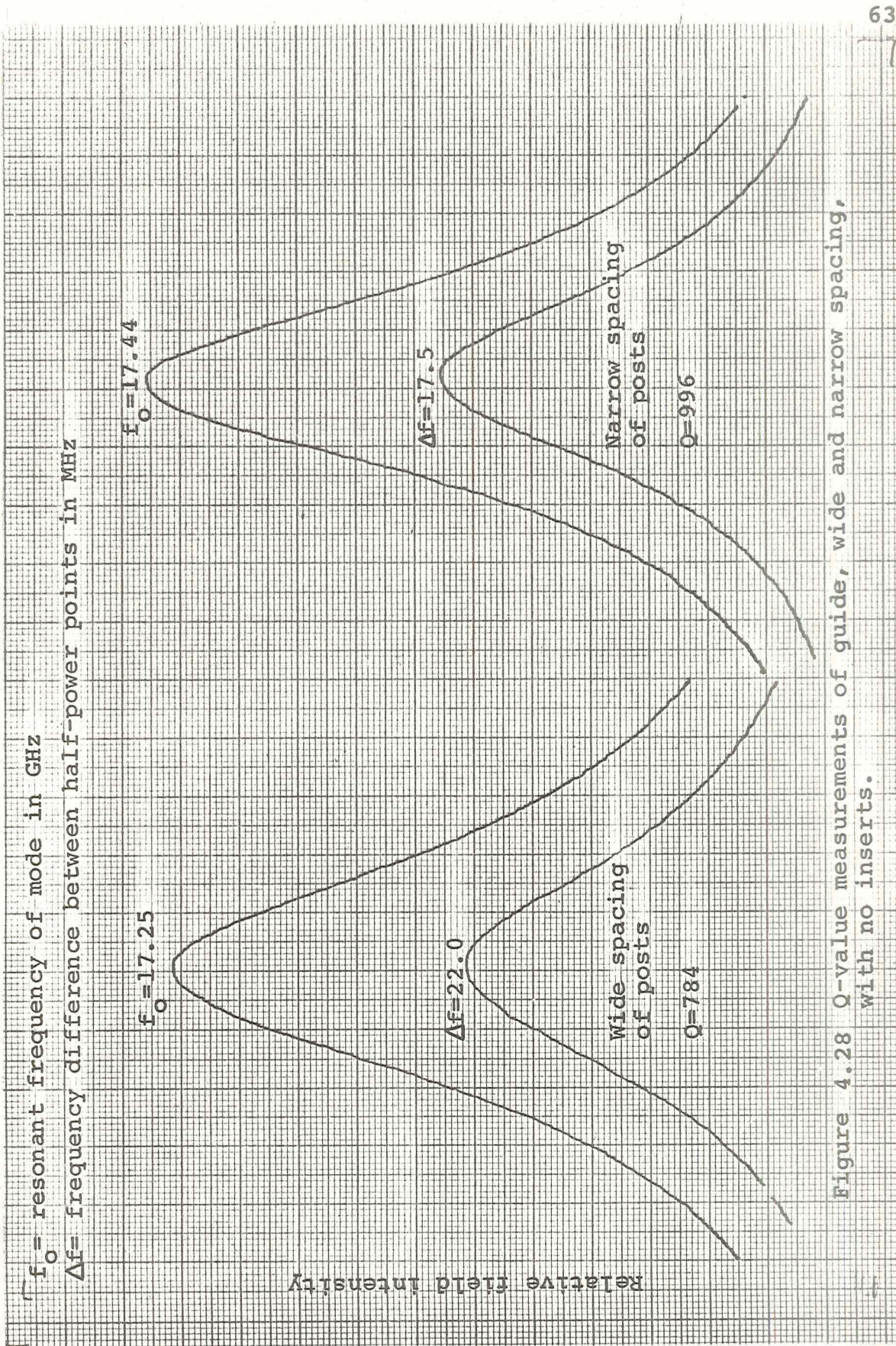


Figure 4.28 Q-value measurements of guide, wide and narrow spacing, with no inserts.



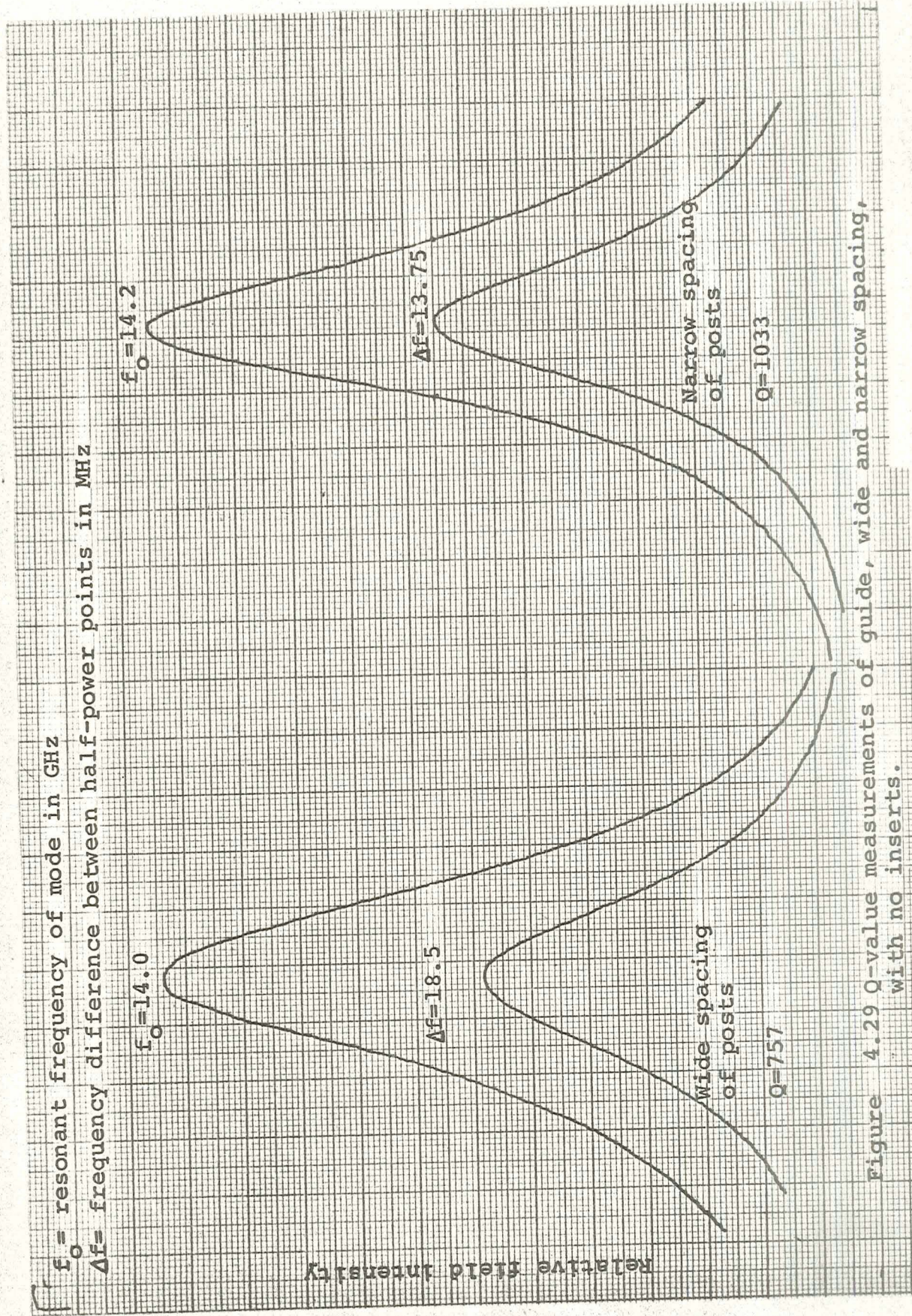


Figure 4.29 Q-value measurements of guide, wide and narrow spacing, with no inserts.



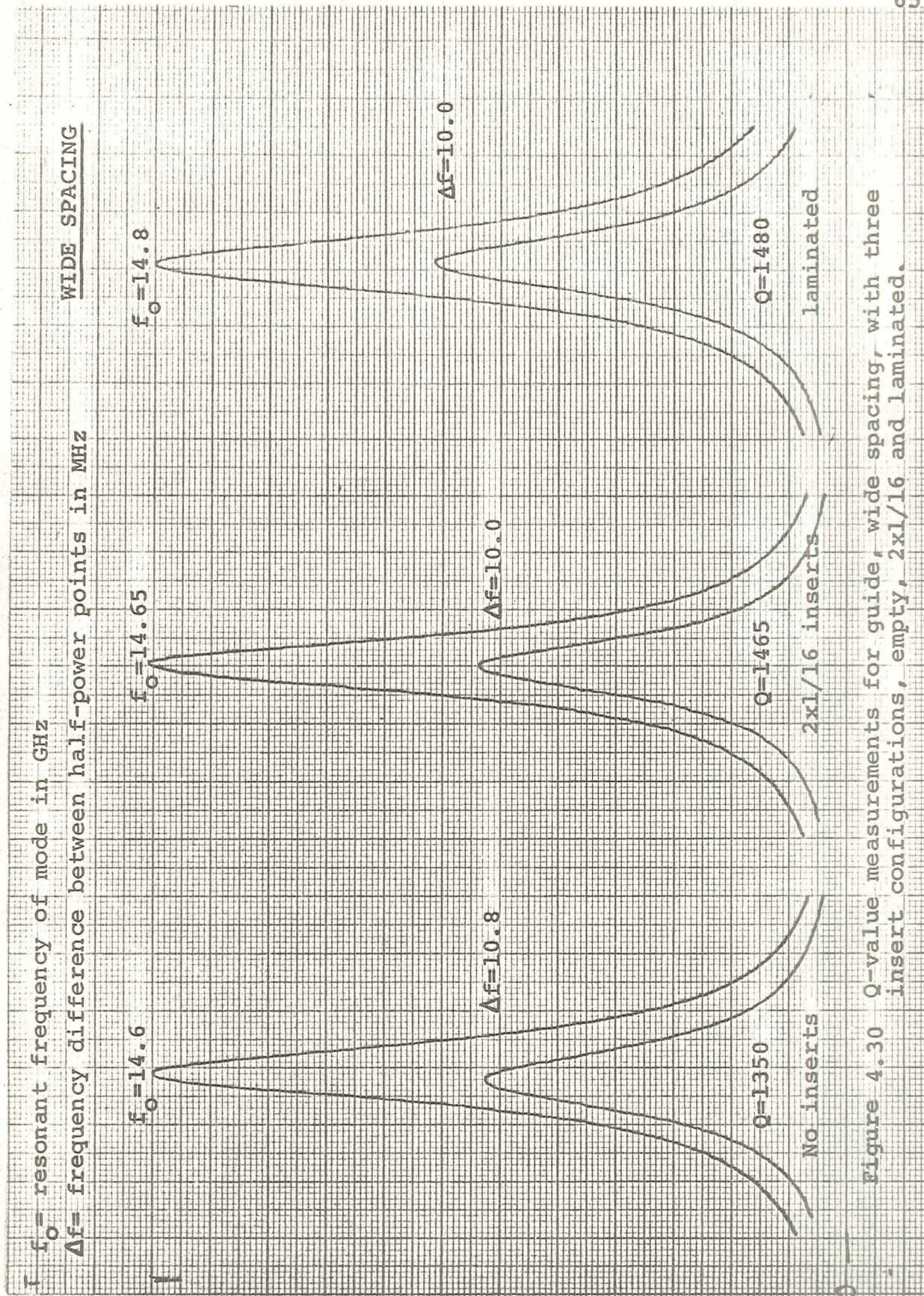


Figure 4.30 Q-value measurements for guide, wide spacing, with three insert configurations, empty, 2x1/16 and laminated.



# WIDE SPACING

$f_o$  = resonant frequency of mode in GHz  
 $\Delta f$  = frequency difference between half-power points in MHz

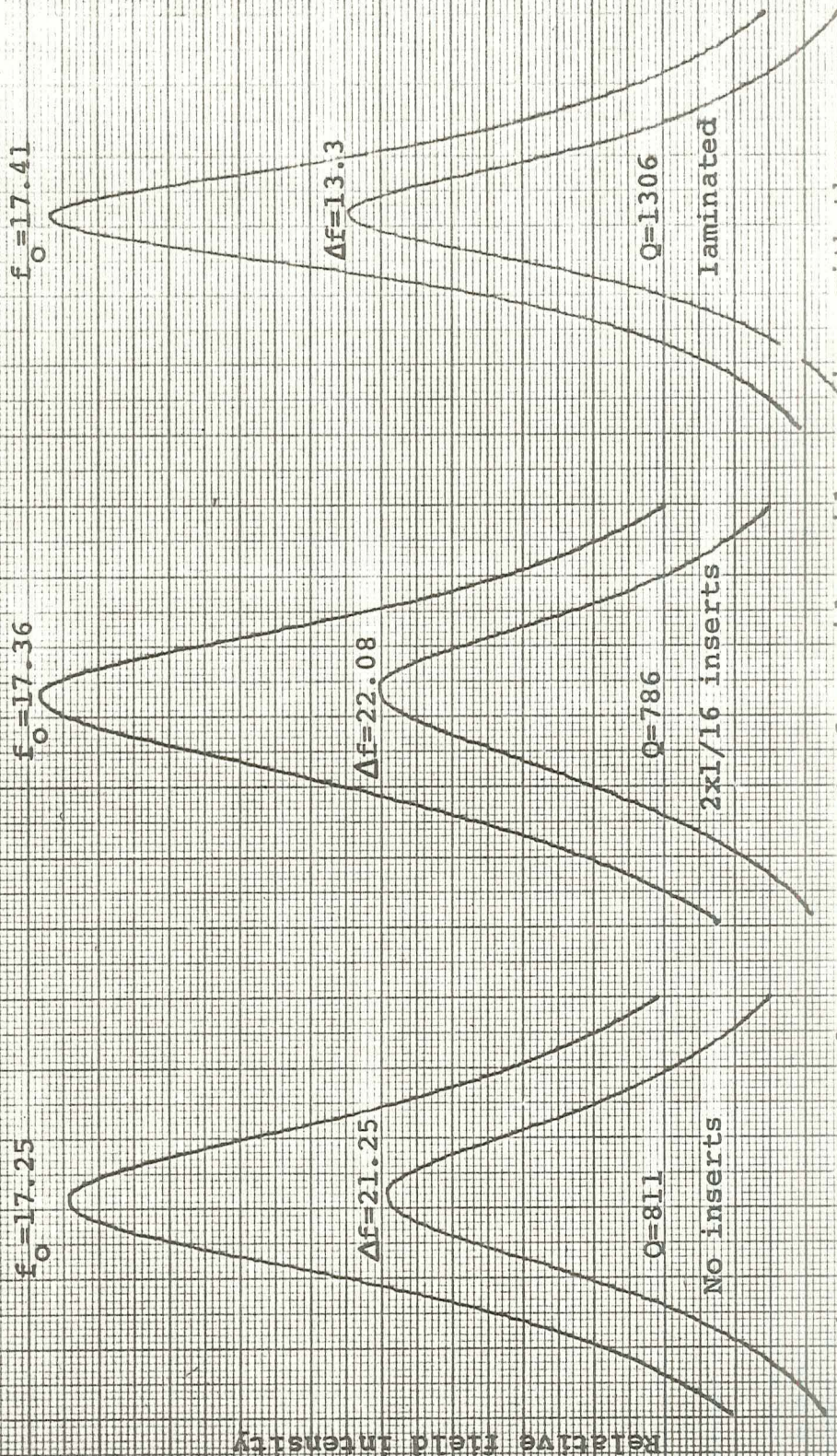


Figure 4.31 Q-value measurements for guide, wide spacing, with three insert configurations, empty, 2x1/16, and laminated.



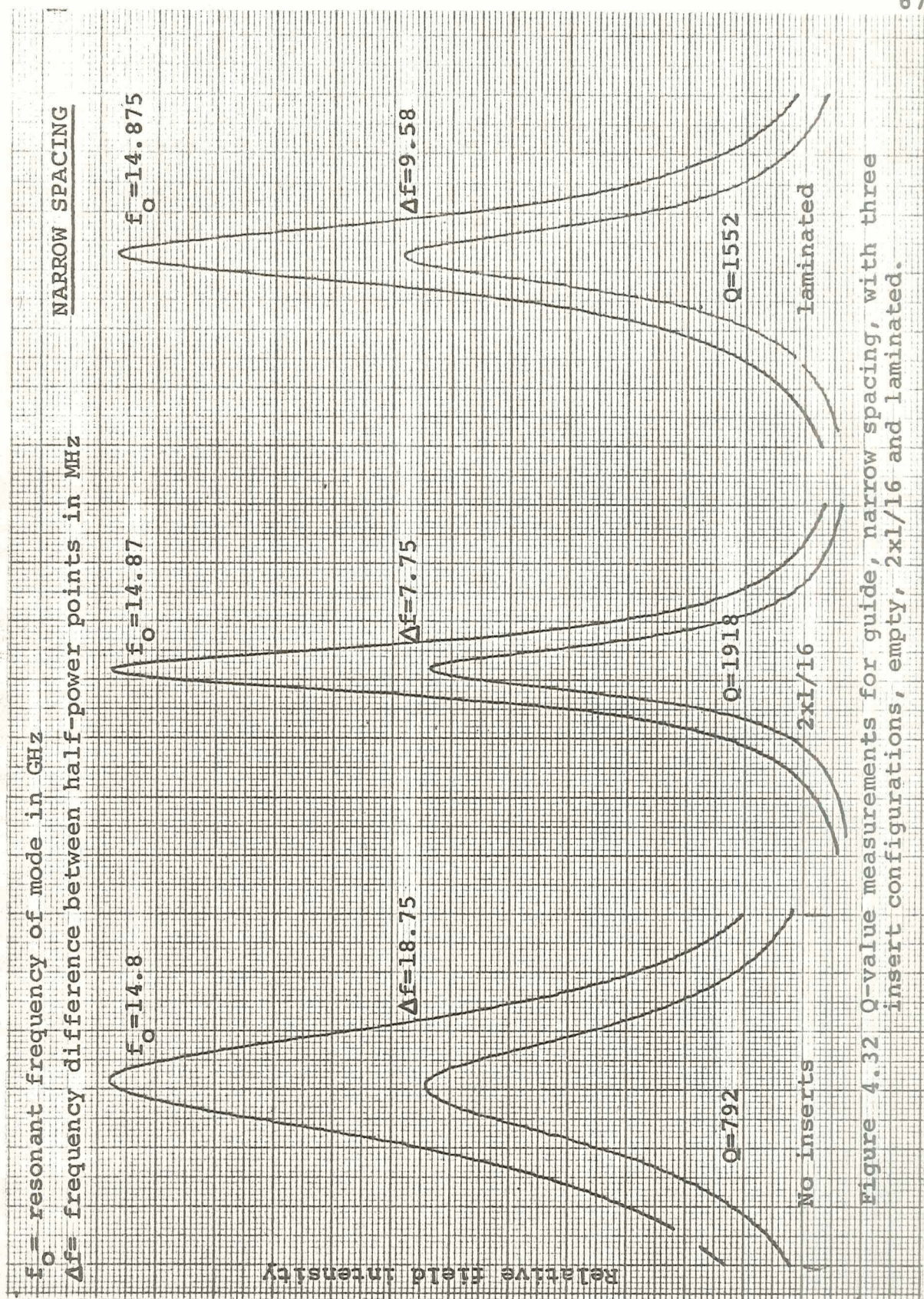


Figure 4.32 Q-value measurements for guide, narrow spacing, with three insert configurations, empty, 2x1/16 and laminated.



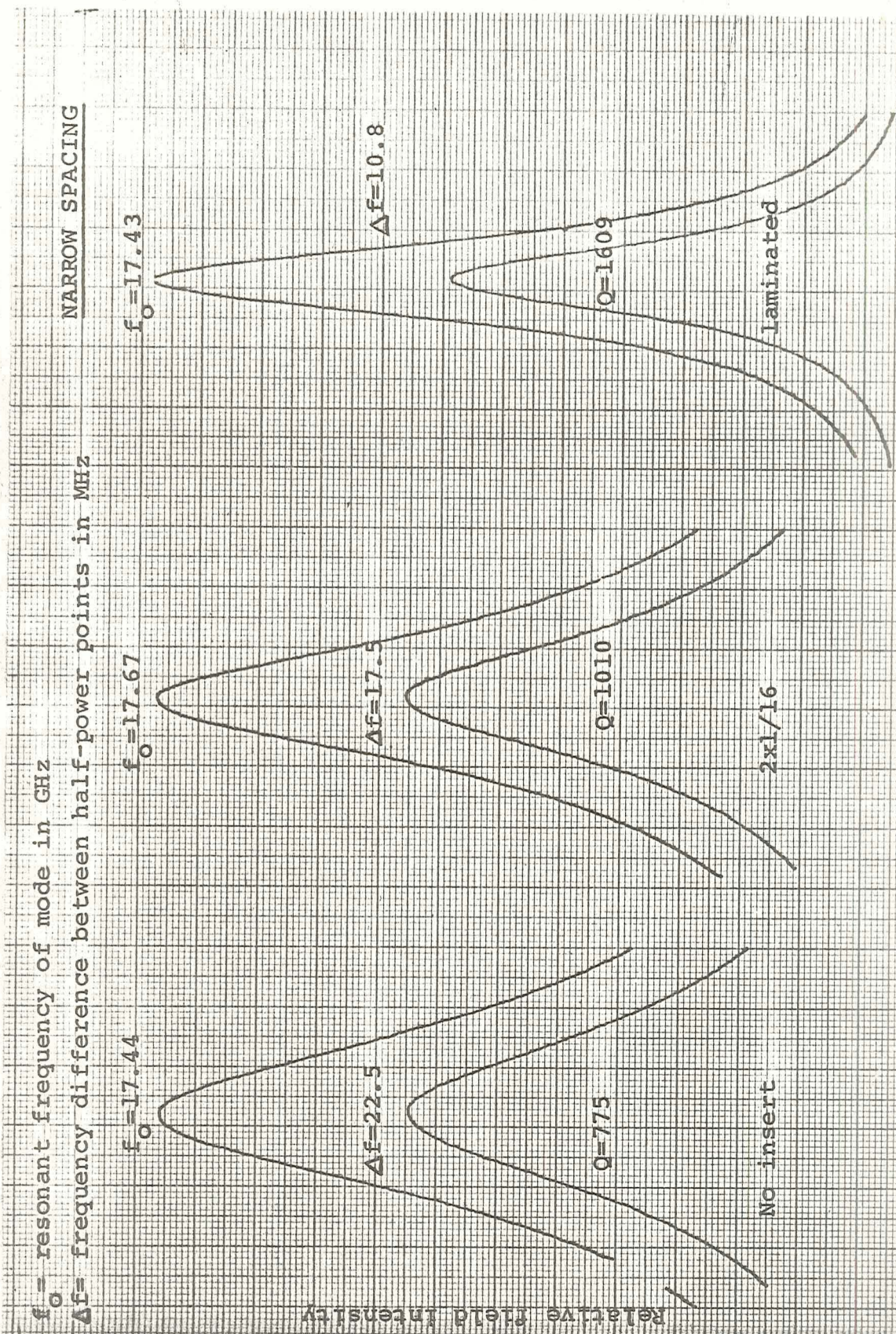


Figure 4.33 Q-value measurements for guide, narrow spacing, with three insert configurations, empty, 2x1/16 and laminated.



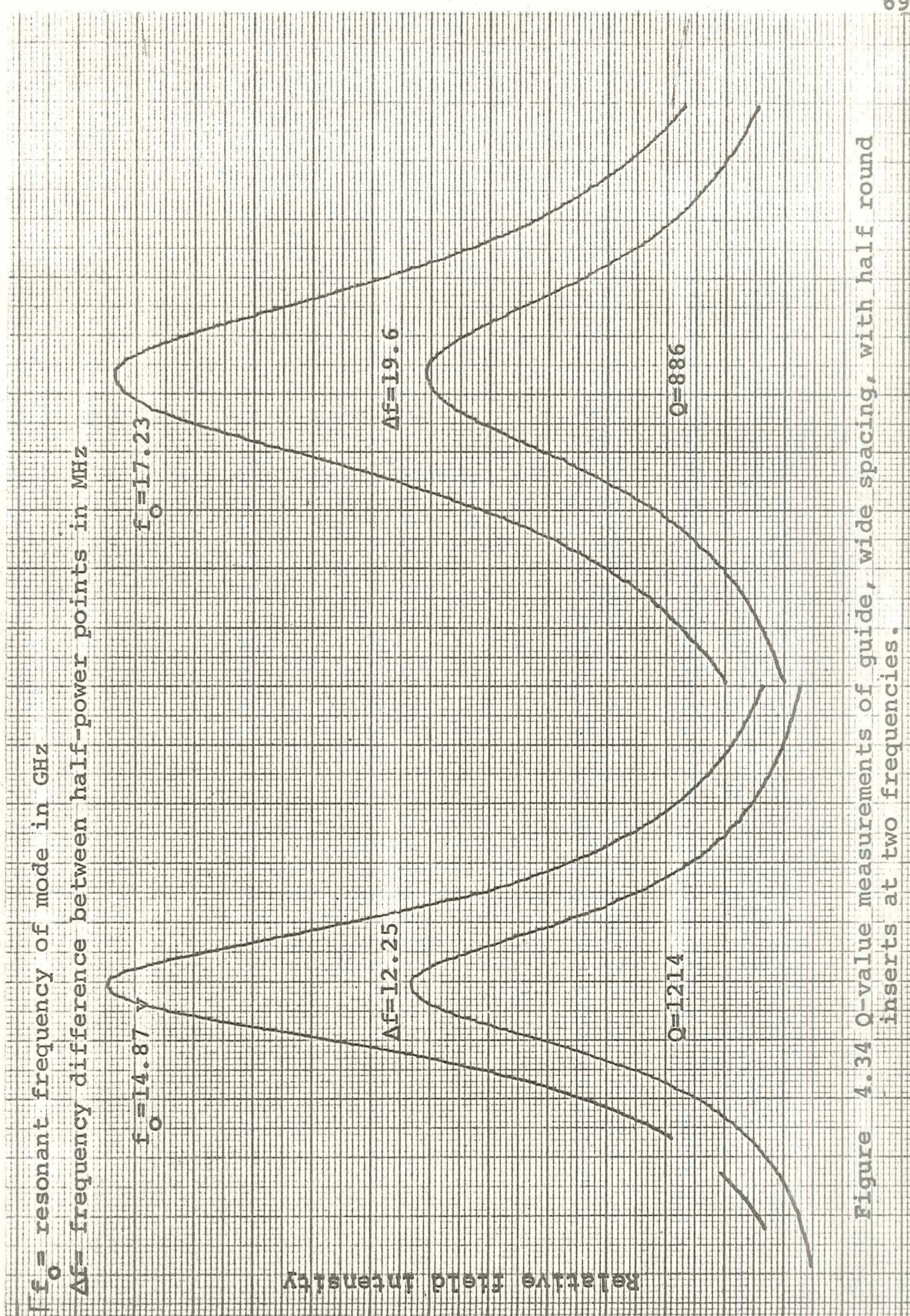


Figure 4.34 Q-value measurements of guide, wide spacing, with half round inserts at two frequencies.



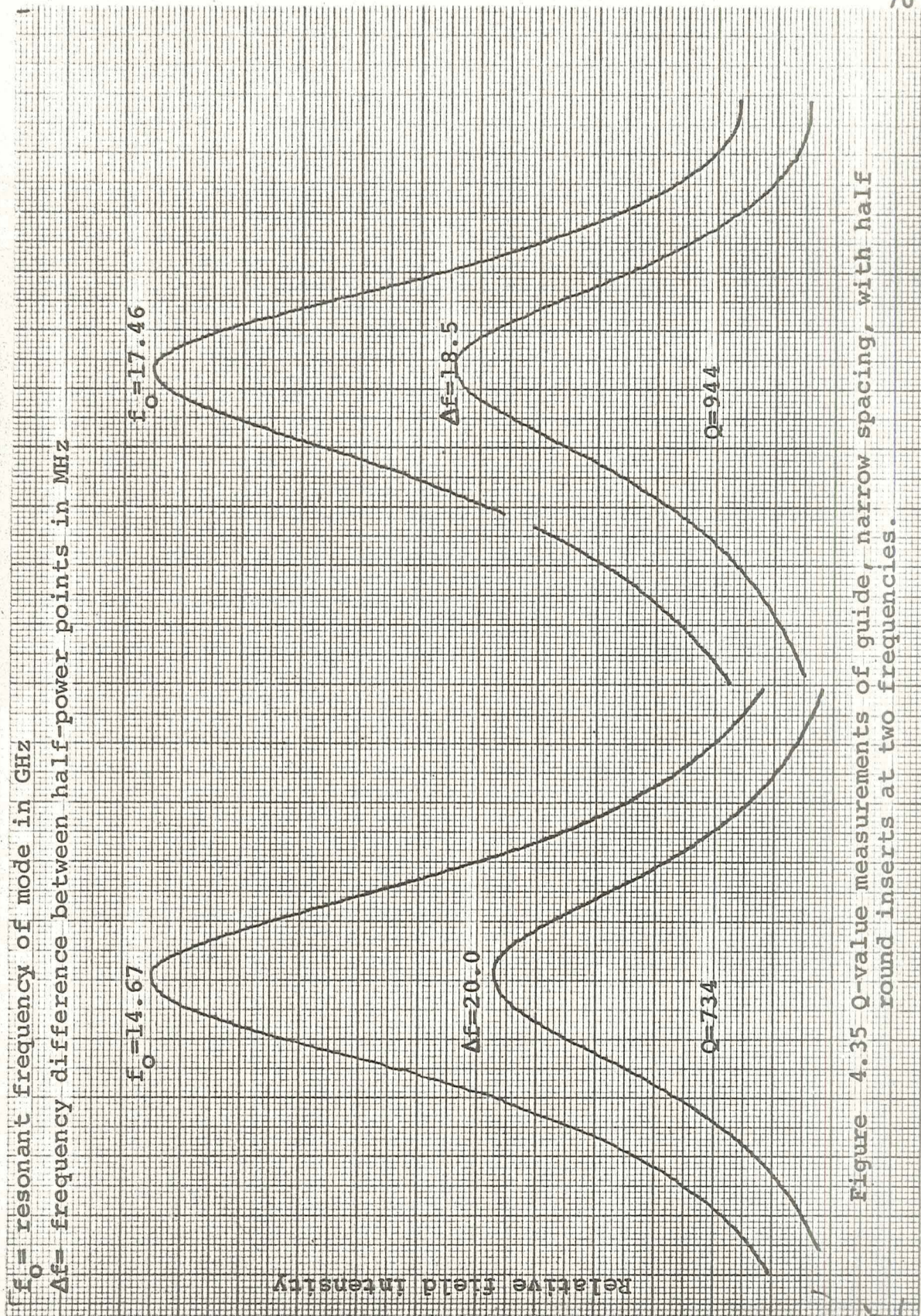


Figure 4.35 Q-value measurements of guide, narrow spacing, with half round inserts at two frequencies.



#### 4.4 Measurement of Lateral Leakage

As an indication of leakage through the fence posts, measurements were made at two frequencies for six configurations. Table 4.6 summarizes the results of these measurements by giving the ratio of the field intensities in dB of the field maximum inside the guide at the bottom center and the maximum field outside the fence, bottom next to the fence.

Figure 4.36 gives a representative plot of the transverse field distribution.



Table 4.6 Energy Leakage

	Wide spacing		Narrow spacing	
	Frequency	Leakage	Frequency	Leakage
Empty	14.65 GHz 15.3	36dB 28	16.8 GHz 16.1	35dB 44
2x1/16	15.13 16.15	28 25	15.27 15.8	45 37
round	16.07 17.07	22 26	16.7 15.9	35 22



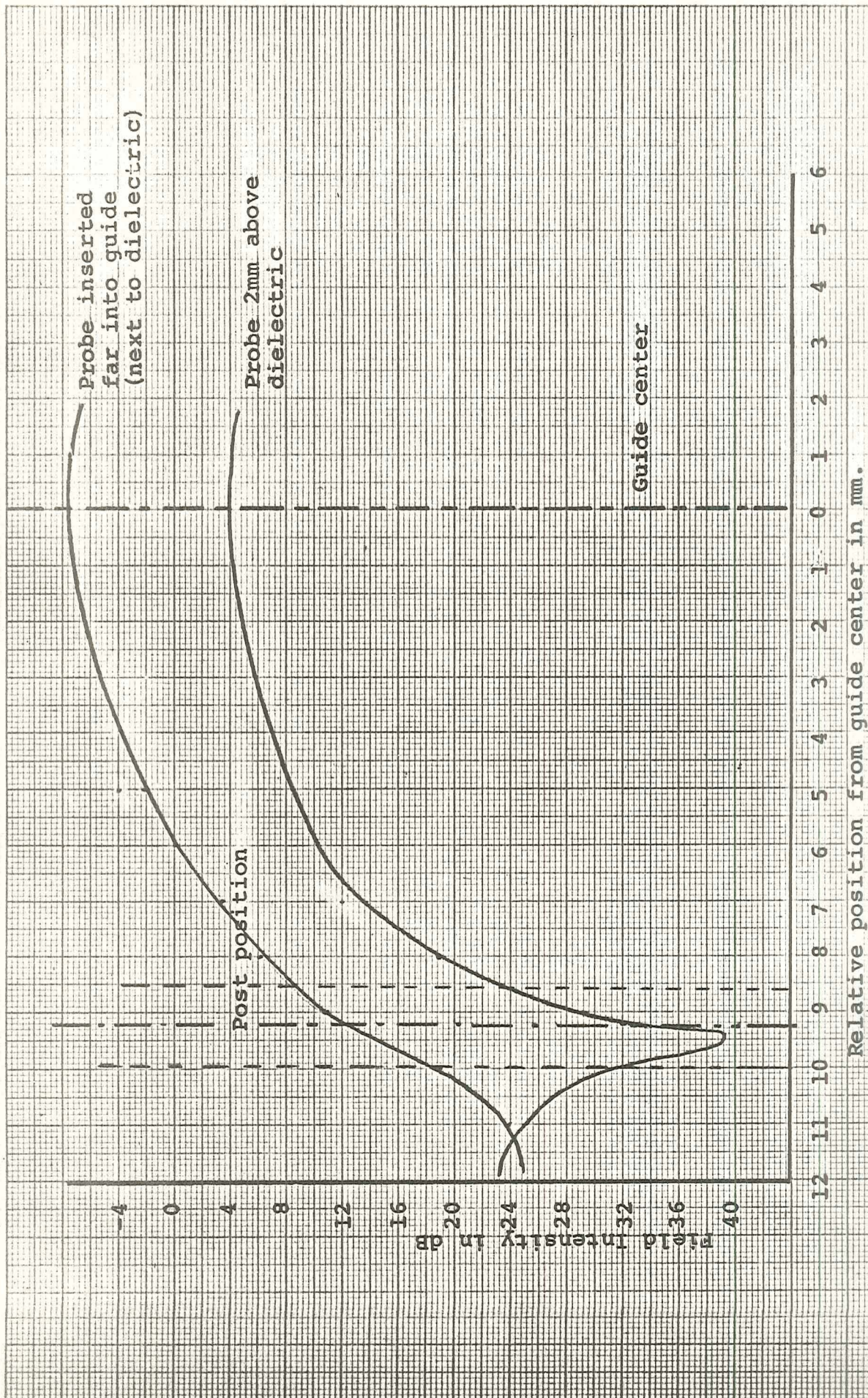


Figure 4.36 Leakage, wide guide, empty. (Note that the probe is small enough to travel through posts.)



## 5. SUMMARY

Due to high attenuation and low power handling capability of conventional rectangular waveguide at millimeter wave frequencies it has become necessary to investigate the properties of non-conventional waveguide structures. The fence-guide is an H-type structure which offers simple fabrication and use of the H-guide structure offers improvements such as reduced attenuation. Investigation of the fence-guide was carried out at 12-18 GHz.

The two prototype fence-guides, with different post spacing, were observed to have different loss characteristics. With increased post spacing an increase in losses was observed. Mode distribution was well defined except for the case of circular inserts. The circular insert mode distributions were too crowded to be measured. The characteristics of the laminated guide were similar to the empty fence guide except for the Q-values which were generally higher for the laminated guide.

The effect of post spacing on exponential decay of the fields was insignificant; however, the dielectric loading had some noticeable effect. The dielectric loading increased the rate of exponential decay.



LIST OF REFERENCES

- Collin, R.E. 1960. Field Theory of Guided Waves. McGraw-Hill Book Company, Inc., New York.
- Griemsmann, J.W.E. and L. Birenbaum. 1959. A low loss H-guide for millimeter wavelengths. Proc. of the Symposium on Millimeter Waves. Polytechnic Institute of Brooklyn, New York: 543-562.
- Lewis, E.A. and J. Casey. 1952. Electromagnetic reflection and transmission by gratings of resistive wires. J. Applied Phy. vol. 23: 605-608.
- Macfarlane, G.G. 1946. Surface impedance of an infinite parallel wire grid at oblique angle of incidence. J. Inst. Elec. Engr. (pt. 3A) vol. 93: 1523-1527.
- Ramo, S., J.R. Whinnery, and T. Van Duzer. 1965. Fields and Waves in Communication Electronics. John Wiley and Sons, Inc. New York.
- Tischer, F.J. 1953. A wave guide structure with low losses. Archiv der Elektrischen Ubertragung 7:592-596.
- Tischer, F.J. 1956. The H-guide, a waveguide for microwaves. I.R.E. Convention Record (Part 5): 44-47.
- Tischer, F.J. 1958. Properties of the H-guide at microwaves and millimeter waves. Wescon Convention Record (Part I): 4-12.
- Tischer, F.J. 1969. Analysis of the multiple strip H-guide. Proc. I.E.E. vol. 116 (No. 9): 1509-1513.
- Wait, J.R. 1954. Reflection at arbitrary incidence from a parallel wire grid. Applied Scientific Research (sec. B) vol. 4: 393-400.